International Journal of Nanomedicine

Dovepress
Taylor & Francis Group

Open Access Full Text Article

ORIGINAL RESEARCH

Green Biosynthesis of Bimetallic Copper Oxide-Selenium Nanoparticles Using Leaf Extract of *Lagenaria Siceraria*: Antibacterial, Anti-Virulence Activities Against Multidrug-Resistant *Pseudomonas Aeruginosa*

Fathy M Elkady[1], Bahaa M Badr[2,3], Ebrahim Saied[4], Amr H Hashem[4], Mostafa A Abdel-Maksoud[5], Sabiha Fatima[6], Abdul Malik[7], Mohammed Aufy[8], Ahmed M Hussein[8], Mohammed S Abdulrahman[1], Hany R Hashem[9]

[1]Microbiology and Immunology Department, Faculty of Pharmacy (Boys), Al-Azhar University, Cairo, Egypt; [2]Department of Basic Medical and Dental Sciences, Faculty of Dentistry, Zarqa University, Zarqa, Jordan; [3]Department of Medical Microbiology and Immunology, Faculty of Medicine, Al-Azhar University (Assiut Branch), Assiut, Egypt; [4]Botany and Microbiology Department, Faculty of Science, Al-Azhar University, Cairo, Egypt; [5]Department of Botany and Microbiology, College of Science, King Saud University, Riyadh, 11451, Saudi Arabia; [6]Department of Clinical Laboratory Science, College of Applied Medical Sciences, King Saud University, Riyadh, 11433, Saudi Arabia; [7]Department of Pharmaceutics, College of Pharmacy, King Saud University, Riyadh, 11433, Saudi Arabia; [8]Department of Pharmaceutical Sciences, Division of Pharmacology and Toxicology, University of Vienna, Vienna, Austria; [9]Department of Microbiology and Immunology, Faculty of Pharmacy, Fayoum University, Al-Fayoum, Egypt

Correspondence: Ahmed M Hussein; Amr H Hashem, Email ahmed.hussein@univie.ac.at; amr.hosny86@azhar.edu.eg

Introduction: Clinical isolates of *Pseudomonas aeruginosa* (*P. aeruginosa*) are among the most recovered bacteria with phenotypic antimicrobial resistance. Bimetallic nanoparticles (BNPs) have received much attention for antimicrobial activity in the last decade. This research aimed to biosynthesize bimetallic copper oxide-selenium nanoparticles (CuO-Se BNPs) and to assess its bioactivity on various *P. aeruginosa* clinical isolates.

Methodology: Based on the possible synergistic effects, CuO-Se BNPs were selected and biosynthesized using leaf extract of *Lagenaria siceraria* (*L. siceraria*) for the first time. The obtained BNPs were characterized using UV-vis spectroscopy, X-ray diffraction (XRD), energy dispersive X-ray spectroscopy (EDX), and transmission and scanning electron microscopes. The capability of Cu-Se BNPs to cease the growth of *P. aeruginosa* isolates and to reduce their virulence characters was evaluated. Also, different cell lines were used to assess its cytotoxicity and anticancer activity.

Results: The elemental composition of CuO and Se was revealed by the UV, XRD, and EDX data, indicating the synthesis of CuO-Se core shell BNPs with a size of 50 nm. In well diffusion assay, CuO-Se BNPs *P. aeruginosa* growth with 10–21 mm inhibition zone diameter and 38–95% inhibition. Also, the minimum inhibitory concentration and minimum bactericidal concentration were in a relatively wide range of 7.8–250 µg/mL and 31.2–500 µg/mL, respectively, with tolerance level range of 2–16. Additionally, CuO-Se BNPs shown anti-pyocyanin activity of 4.35–63.21% inhibition while the anti-proteolytic activity was in a range of 4.96–12.59% and anti-pyoverdine effect was in a range of 0.24–83.41%. The IC50 against Wi-38 normal cells was 267.2 µg/mL while the IC50 were 31.1 and 83.4 µg/mL against MCF-7 and Hep-G2, respectively, indicating promising anticancer activity.

Conclusion: This research demonstrates the promising antibacterial, anti-virulence, and antitumor properties with safe low concentrations of CuO-Se NPs, synthesized via an eco-friendly green synthesis method without the use of toxic chemicals, offering a sustainable and cost-effective alternative.

Keywords: bimetallic nanoparticles, *P. aeruginosa*, MIC, anti-virulence activity, anticancer impacts

Received: 16 October 2024
Accepted: 20 March 2025
Published: 14 April 2025

Introduction

Antimicrobial resistance amongst *P. aeruginosa* isolates is a global threat with major importance due to its ability to cause a wide range of serious hospital-acquired infections. This pathogen represents one of the Gram-negative superbugs with distinctive adaptability, opportunistic character, and complicated antimicrobial resistance mechanisms.[1]

Additionally, *P. aeruginosa* showed increased resistance to colistin, the last resort for controlling the bacterial antimicrobial resistance.[2] The virulence factors of *P. aeruginosa* were categorized as those involved in alteration of the bacterial surface structures, factors required for bacterial cell-to-cell communication including quorum sensing (QS) and biofilm formation, and the secreted factors including proteases, siderophores, and toxins.[3,4] Clearly, the severe *P. aeruginosa* infections are associated with bluish green pyocyanin toxic secondary metabolite production. This toxic pigment diminishes lung function through its free radical and pro-inflammatory promoting activity.[5]

Also, the zinc-dependent elastase LasB is a member of the secreted virulence factors with proteolytic and elastolytic activities which that proceed proceeds the host cells colonization by *P. aeruginosa*. This enzyme dissolves the host connective tissue and inactivates the host proteins involved in defense mechanisms. The development of pathoblockers targeting LasB is of great concern as a new mechanism that counteracts the *P. aeruginosa* virulence.[6] Additionally, the free iron in the human body is naturally restricted to the lactoferrin. This protein chelates the iron with consequent prevention of *P. aeruginosa* aggregation and biofilm creation, which is encouraged by type IV twitching motility.[7] Unfortunately, the proteases protease enzymes secreted by *P. aeruginosa* digest the lactoferrin with consequent free iron liberation. As well, the yellowish green fluorescent pigment pyoverdine and pyochelin iron chelating siderophores help the *P. aeruginosa* to utilize its iron requirement from the surrounding environment.[8]

Nanotechnology can precisely construct materials and devices by precisely controlling three-dimensional molecular structures.[9,10] It also provides a novel, reliable, and adaptable drug delivery platform that helps overcome the drawbacks of traditional chemotherapy.[11] The numerous benefits that NPs provide in the therapy of cancer include their tiny size, high surface-to-volume ratio, distinctive fluorescence characteristics, enhanced permeability, and exceptional biocompatibility.[12,13] Metallic NPs function better than other NPs and have a great deal of promise for use as pharmacological agents.[14] Bimetallic NPs have garnered a lot of attention in the past 10 years because of their distinct optical, electrical, magnetic, and catalytic characteristics, which are generally distinct from those of their monometallic counterparts. Since they often exhibit greater activity, selectivity, and stability than monometallic NPs, BNPs, which are made up of two distinct metal elements, have acquired significance.[15]

Bimetallic NPs usually exhibit more interesting properties than their comparable monometallic NPs because of the synergistic properties between the two distinct metal components.[16] The synergistic properties between the two distinct metal components in BNPs usually exhibit more interesting properties than their comparable monometallic NPs.[16] In contrast to chemical and physical approaches, however, the biosynthesis of BNPs is a safe, cheap, environmentally friendly, clean, and green process.[17] BNPs have been reported to exhibit superior antimicrobial properties compared to monometallic NPs. The interaction between two different metals can enhance the antimicrobial effect by generating more reactive species or by disrupting the microbial cell structure more effectively. Numerous eco-friendly techniques for creating different kinds of bimetallic NPs in solution have been revealed.[18] Environmental problems, such as hazardous trash and harmful water contamination, have drawn a lot of attention lately.[19] In contrast to chemical and physical approaches, however, the biosynthesis of BNPs is a safe, cheap, environmentally friendly, clean, and green process.[17] There is currently a need to create low-cost, accessible, scalable, and straightforward techniques for acquiring NPs. These objectives are met by plant extracts since they are environmentally benign, renewable, and simple to grow on a large scale. Phytochemicals have two functions in the creation of metallic NPs:[20] they act as a reducing agent, and they stabilize the NPs.[21,22] Bimetallic NPs synthesis mediated by plants are more stable and come in a variety of sizes and shapes. Therefore, the synthesis of BNPs depends on the reducing agent in the plant extract (flavonoids, terpenoids, and phenolic acid).[23] Flavones, isoflavones, flavonols, anthocyanins, and flavonoids are the most well-known polyphenols found in a wide variety of fruits and vegetables. Lignans are plentiful in cabbage, broccoli, carrots, or grains, whereas phenolic acids, including gallic, syringic, and salicylic acids, are found in many plant species.[24,25] Large, softly pubescent, annular, ascending, or trailing, *L. siceraria* is a herb that grows all over the world. In ethnic medical systems,

the entire plant is acknowledged to be useful. Physiologically active polysaccharides may be produced by the plant.[26] It is used for both food and medicine because it is a household plant. Several parts of this plant have been studied for their cardioprotective, antidepressant, antihyperglycemic, antimicrobial, cytotoxic, anti-inflammatory, antihyperlipidemic, anti-urolithiasis, antianxiety, analgesic, anticancer, diuretic, anthelmintic, antihepatotoxic, anthelmintic, antistress, immunomodulatory, antiulcer, hepatoprotective, and antioxidant properties.[27–29] It can treat dry cough, muscle soreness, and blood disorders. The hydroxyl, carboxyl, and amino functional groups found in their phytochemicals can be used as capping agents to give the metal NPs a robust coating in a single step as well as efficient metal-reducing agents.[30,31]

As a crucial micronutrient, copper is involved in several enzymatic processes in both plants and animals.[32] Copper NPs have several uses, including the treatment of plant diseases, electronics, coating fabrics, and antibacterial applications.[33] Recently, scientists have successfully produced biogenic NPs using various plant extracts.[34,35] Anticancer treatment may benefit from the use of selenium in NPs (SeNPs).[36] Although SeNPs exhibit remarkable anti-tumor action, their limited stability and facile aggregation limit their use.[37] Bimetallic NPs are therefore made by combining two metal NPs with distinct structural properties to circumvent the drawbacks of dealing with single-metal NPs.[38] Bimetallic NPs' unique geometrical structure and mixing pattern make them more useful. Bimetallic NPs have outperformed their monometallic counterparts in several areas, including durability and activity, and they do so without the requirement for expensive or specialist equipment.[39]

Herein, this research aimed to biosynthesize the CuO-Se BNPs using leaf extract of *L. siceraria* for the first time. Also, to evaluate its effect on *P. aeruginosa* toxin formation, secreted virulence factors production, and consequent quorum sensing as well as its cytotoxicity on Wi-38 normal cell line and anticancer activities against MCF-7 and Hep-G2 cell lines.

Materials and Methods

Clinical Isolate and Its Virulence Characters

A total of 24 phenotypically identified *P. aeruginosa* clinical isolates from patient with infected wound were included in our current study. These isolates were gained from the microbiology lab at Sayed Galal University hospital, Al–Azhar University, Cairo, Egypt, and identified as 3 non-biofilm forming isolates and 21 isolates with different levels of biofilm formation. In all experiments of our research, each tested isolate suspension was adjusted to 1 X 10^8 CFU/mL equivalent to 0.5 McFarland standard turbidity using several pure bacterial colonies from fresh culture in autoclave sterilized 0.9% normal saline.

Pyocyanin Production

In 250 mL flask, 50 mL nutrient broth supplemented with 1% glycerol was aseptically inoculated with each tested *P. aeruginosa* strain to assess its pyocyanin pigment production ability. Incubation was carried out with shaking at 150 rpm at 37°C for 72 h. Typically, pyocyanin pigment production manifested by a blush green color with different intensity according to the production level.[40]

Total Proteases Evaluation

The casein agar plate method was applied for initial examination of *P. aeruginosa* total proteases production. Each tested bacterial isolate was aseptically streaked onto skim milk agar medium containing defatted milk granules (10%), nutrient broth (25%), and agar (2%). After incubation for 24 h at 37°C, bacterial growth with surrounded clear zone was considered as a positive proteolytic test.[41]

Preparation L. Siceraria Leaf Extract

Leaves of *L. siceraria* were collected from Giza Governorate, Egypt (29°47′35″N 31°13′51″E).

The plant was identified by Prof. Dr. Abdou Marie Hamed from the Botany and Microbiology Department, Faculty of Science, Al-Azhar University, Cairo, Egypt with Voucher no. 912. The experimental research and field studies, including the collection of plant material, were conducted in compliance with the relevant institutional, national, and international guidelines and legislation.

After washing with tap water to get rid of any dirt or undesired items, leaves were washed with double-distilled water and left to air dry at room temperature. In a 250 mL round-bottom flask, 200 mL of double-distilled water was combined with 10 g of finely ground leaves, and the mixture was refluxed for 60 min. For further processing, the extract was cooled to room temperature and filtered through Whatman filter paper number 1.[42]

Biogenic Synthesis of CuO-Se BNPs

Copper acetate and sodium selenite were obtained from Sigma-Aldrich, Cairo, Egypt. Ten milliliters of 5 mm sodium selenite and 10 mL of 5 mm copper acetate were combined and stirred at room temperature for approximately 8 min, a blue colloid developed at room temperature. A dark green solution was obtained by adding 80 mL of the prepared *L. siceraria leaf extract* to them which prepared by heating it to 90°C for one hour. The mixed solution exhibited a final pH of 8.0. The synthesis of CuO-Se BNPs was carried out under continuous agitation at 250 rpm in a shaking incubator for approximately 24 hours, with the incubation temperature maintained at 35°C. After that, the reaction mixture was centrifuged for 5 min at 10,000 rpm to get rid of the metal precursors and inert plant material. The solid material was subjected to several meticulous washings using ethanol and deionized water prior to being dried for a duration of 48 h at a temperature of 50°C and then kept in a cool atmosphere.[43]

Characterization of CuO-Se BNPs

Numerous spectral techniques, such as SEM, DLS, TEM, XRD, FTIR, UV-vis spectroscopy, and EDX spectroscopy, were available to characterize the biogenically synthesized CuO-Se BNPs.[44] These analyses were conducted at the Desert Research Center in Cairo, and the UV measurements were performed at the Faculty of Science, Al-Azhar University for Boys.

Examination of CuO-Se BNPs Antibacterial Activity

Various anti-pseudomonas activity of the biosynthesized CuO-Se BNPs was assessed via well diffusion, broth microdilution, antitoxin, and crystal violet (CV) assays.

Well Diffusion Method

The activity of the biosynthesized CuO-Se BNPs against *P. aeruginosa* clinical isolates was investigated following the agar well diffusion assay.[45] Each pure bacterium suspension from overnight culture on nutrient agar medium at 37°C, was inoculated onto Mueller Hinton agar (MHA) plate by sterile cotton-tipped swab to create a confluent bacterial growth. Consequently, five equidistance wells were made on the agar surface using sterile borer. An amount of 80 µL of the tested BNPs suspended in dimethyl sulfoxide (DMSO) at a concentration of 2000 µg/mL was added to the first well. The remaining wells were then filled with copper acetate (100 µg/mL), sodium selenite (100 µg/mL), ceftriaxone (50 µg/mL) as a positive control, and DMSO (8%) as a negative control (NC). All plates were kept in the refrigerator for 30 min to allow the NPs suspension pre-diffusion into the MHA followed by aerobic incubation for 24 h at 37°C. The experiments were conducted as triplicate and the measured inhibition zone diameter (IZD) around wells containing NPs were shown as the mean ± standard deviation (mean ± SD). To correlate the findings to ceftriaxone standard activity, the CuO-Se BNPs activity index (AI) was calculated according to formula (1), while the percent inhibition (PI) was calculated according to formula (2) as described by.[46]

$$\text{Activity Index (AI)} = \frac{\text{IZD caused by the BNPs}}{\text{IZD caused by the standard antimicrobial}} \quad (1)$$

$$\text{Percent Inhibition (PI)} = \text{AI} \times 100 \quad (2)$$

Assessment of Inhibitory Concentrations

The quantitative ability of CuO-Se BNPs to cease the growth of the tested *P. aeruginosa* clinical isolates and subsequently bacteriostatic or bactericidal activity evaluation was determined according to.[47] The broth microdilution assay was performed to find out the minimum inhibitory concentration (MIC). In brief, the stock concentration of 4000 µg/mL

was prepared by dissolving 4 mg of biosynthesized BNPs in 1 mL DMSO. Fifty microliters from the biosynthesized NPs stock concentration was added to the 1st well in each row of the 96-well microtiter plates containing 50 µL tryptic soya broth (TSB) followed by 2–fold serial dilution performance. Bacterium inoculum (10 µL) was then added to each well followed by TSB to 200 µL as a final volume. Well containing TSB, DMSO, and tested bacterial isolate without BNPs suspension was used as a positive control, while the well representing the negative control test contained TSB, DMSO, and BNPs without bacterial suspension. After 24 h incubation at 37°C, 0.015% resazurin solution (40 µL) was transferred to each well followed by incubation for 2 h at 37°C. The lowest concentration of the NPs associated with no color change into red was considered as the MIC. The suspension from each well containing MIC and other higher concentrations of the NPs were inoculated onto MHA plate. After overnight incubation at 37°C, the lowest concentration of the NPs showed no bacterial growth was scored as the minimum bactericidal concentrations (MBC). Afterward, the tolerability of each P. *aeruginosa* clinical isolates was calculated as described by antibacterial activities of the extracts, fractions and isolated compounds from Canarium patentinervium Miq. against bacterial clinical isolates | BMC Complementary Medicine and Therapies | Full Text following the formula (3).

$$\text{Tolerance level} = \frac{\text{MBC}}{\text{MIC}} \tag{3}$$

The tolerance level of the CuO-Se BNPs ≤4 illustrates its ability for bacterial cells destruction and bactericidal effect. In contrast, tolerance level > 4 indicates its limited ability for growth inhibition only and bacteriostatic effect.

Anti-Virulence Factors Assays

The *P. aeruginosa* bacterial cell-free supernatant was prepared. In brief, each tested strain was cultured in glucose-enriched LB broth (30 mL) and incubated aerobically for 24 h at 37°C with shaking at 180 rpm. The bacterial un-inoculated broth was used as a negative control (NC). The supernatant obtained by centrifugation for 15 min at 10,000×g was discarded. The fresh glucose-enriched LB broth (30 mL) was used to re-suspend the obtained bacterial pellet followed by addition of 0.5 MIC of the tested BNPs (T). The BNPs untreated bacterial suspension was used as positive control (PC). Each flask was entirely covered with aluminum foil to avoid pyocyanin breakdown and incubated aerobically for 24 h at 37°C with shaking at 180 rpm. The cell-free supernatant, from T, PC, and NC tests, was collected by centrifugation for 15 min at 10,000×g, sterilized via syringe filter (0.22 µm), and stored at 4°C for quantitative pyocyanin and total protease production assays.

The CuO-Se BNPs effect on pyocyanin pigment was quantitatively estimated according to the method described by.[48] In brief, 15 mL from the collected T, PC, and NC tests supernatant was mixed with 9 mL of chloroform with vortexing until the color changed into greenish blue. The obtained mixture was centrifuged for 10 min at 10,000×g, the blue chloroform containing phase (at the bottom) was separated, and the process was repeated three times. The obtained blue colored liquid (6 mL) was then mixed with 3 mL of 0.2M HCl in a new tube followed by shaken until the original blue color changed into pink, the process was repeated three times. The absorbance of the collected pink liquid was measured at 520 nm, multiplied by factor 17.072 to give the pyocyanin concentration (µg/mL) and the pyocyanin percentage inhibition was calculated according to formula (4).

$$\text{Pyocyanin inhibition}(\%) = 1 - \frac{\text{Pyocyanin produced by NC} - \text{Pyocyanin produced by T}}{\text{Pyocyanin produced by PC} - \text{Pyocyanin produced by NC}} \times 100 \tag{4}$$

The biosynthesized CuO-Se BNPs inhibitory effect on *P. aeruginosa* total protease secretion was analyzed following the method described by.[49] In brief, 1 mL of 1.5% skimmed milk was mixed with 5 mL of the obtained T, PC, and NC tests cell-free supernatants followed by incubation at 37°C for 2 h. The tested mixtures (200 µL each) were then separately added to wells of 96-wells microtiter plate. The OD was measured at 500 nm and the inhibition percentage (%) of protease activity was calculated following formula (5).

$$\text{Protease inhibition } (\%) = 1 - \frac{\text{Mean OD of NC} - \text{Mean OD of T}}{\text{Mean OD of PC} - \text{Mean OD of NC}} \times 100 \tag{5}$$

Additionally, the effect of the biosynthesized CuO-Se BNPs on quantitative pyoverdine production was evaluated spectrophotometrically as described by Naik et al.[50] In brief, in presence (T) or absence (C) of 0.5 MIC of the prepared CuO-Se BNPs, each tested isolate was cultured in Muller Hinton broth to the late stationary phase (recorded at OD 600 nm = 0.3). Then, the bacterial cultures were centrifuged for 2 min at 10,000×g and the absorbance of each T and C tests cell-free supernatants was measured at 405 nm and pyoverdine concentration was calculated via its corresponding extinction coefficient (1.9×10^{-4} M^{-1} cm^{-1}) using formula (6).

$$\text{Molar pyoverdine concentration} = \frac{\text{Absorbance at 405 nm}}{\text{Extinction coefficient}} \tag{6}$$

The effect of the prepared CuO-Se BNPs on *P. aeruginosa* pyoverdine production was then calculated according to formula (7).

$$\text{Pyoverdine inhibition}(\%) = 1 - \frac{\text{Pyoverdine concentration in (T)}}{\text{Pyoverdine concentration in (C)}} \times 100 \tag{7}$$

Anti-Biofilm Assay

A CV assay, in microtiter plate, was used to evaluate the biofilm inhibitory effect of 0.5 MIC of the biosynthesized CuO-Se BNPs on *P. aeruginosa* isolate.[51] Briefly, each isolate, with the ability to form bacterial biofilm, was cultured in sterile LB broth supplemented with 2% glucose followed by overnight incubation at 37°C. The tested bacterial suspension was diluted 1:100 and inoculated into the well of the microtiter plate. Ten microliters from the BNPs was then added (T). Each assay was conducted in triplicate and BNPs untreated bacterial culture was included as a control (C) test. After overnight incubation of the microplate, the content of the wells was discarded followed by washing three times using phosphate buffered saline. The adherent biofilm cells in the T and C tests were then stained with CV (0.4%). After incubation for 20 min at 37°C, the excess CV was removed, washed three times with PBS, and 95% ethanol (200 µL) was then added solubilize the remaining CV in the well. The optical density (OD) of the suspension in each well, which reflects the bacterial biofilm intensity, was recorded at 590 nm and the biofilm reduction percentage was calculated using formula (8).

$$\text{Biofilm reduction } (\%) = 1 - \frac{\text{Mean OD590 of BNPs treated biofilm cells}}{\text{Mean OD590 of untreated biofilm cells}} \times 100 \tag{8}$$

Cytotoxicity and Anticancer Activity

The cytotoxicity assay was conducted following the 3-(4,5-dimethylthiazol)-2,5-diphenyl-tetrazolium (MTT) assay described by.[52] The normal human diploid cell line (WI-38) or breast cancerous cell line (MCF-7) and hepatocellular carcinoma cell line (Hep-G2), obtained from the American Type Culture Collection (ATCC), were used for assessment of biosynthesized CuO-Se BNPs cytotoxic or anticancer effects, respectively. The obtained cells OD at 560 nm was used to calculate the cell viability and inhibition percentage, according to the formula (9) and (10), respectively:

$$\text{Viability } (\%) = \frac{\text{Test OD}}{\text{Control OD}} \times 100 \tag{9}$$

$$\text{Inhibition } (\%) = 100 - \text{Viability } (\%) \tag{10}$$

Statistical Analyses

The recorded mean and standard deviation of the results for experiments performed in triplicate were calculated via the Microsoft Excel 2019 software. The frequency and percentage, as a descriptive statistic, were used for our data analysis. SPSS (Statistical Package for the Social Sciences) version 8.0 was applied. The *P* values based significant difference between groups was determined using the one–way ANOVA where the *P* value <0.05 was considered.

Results and Discussion

Virulent Properties P. Aeruginosa Clinical Isolates

The anti-proliferative activity of a virulent determinant, pyocyanin, produced by *P. aeruginosa* can delay recovery from illness caused by this pathogen.[53] Concerning the pyocyanin pigment production, 7/24 (29.2%) of our *P. aeruginosa* isolates (Table 1) showed variable blush green color intensity (Figure 1A) which clarifies their different pyocyanin biosynthesis capability. In a similar study, 45.6% of *P. aeruginosa* clinical isolates were recorded as pyocyanin pigment producers.[54] Also, 22% of the tested *P. aeruginosa* isolates beaten the PAO1 in pyocyanin production, while 42% producing less pyocyanin amount.[55] As well,[56] study reported the ability of 25% of their *P. aeruginosa* clinical isolates for pyocyanin production. Furthermore, variable pyocyanin pigment production rates, 15.7%, 26.3%, or 31.5%, were demonstrated by *P. aeruginosa* clinical isolates cultured on MacConkey agar, blood agar, or nutrient agar, respectively.[57] These heterogenic findings of *P. aeruginosa* pyocyanin isolates production could be attributed for the produced amount of AHL regulating pyocyanin biosynthesis as well as, the culture media and incubation conditions including oxygen tension, pH, and temperature.

Regarding total protease production, the colonies of 8/24 (33.3%) tested isolates (Table 1) grown on skim milk agar showed a clear zone of protein lysis (Figure 1B) illustrating the positivity of their proteolytic activity. In a related study, 20% of the tested *P. aeruginosa* clinical isolates were phenotypically identified as extracellularly protease producer,[55,58] reviewed *P. aeruginosa* arsenal of proteases that associated with its pathogenicity and virulence and consequently its ability to cause a variety of clinical infections.

Biosynthesis of CuO-Se BNPs

For the safe, quick, and inexpensive production of NPs, an eco-friendly substitute for physical and chemical processes might be the use of a biological mass, such as plant extracts or biomass.[59] In the current work, the primary reducing and stabilizing agent used in the phytosynthesis of CuO-Se BNPs was leaf extract. During the reduction reaction, the extract turned dark green, which indicated the formation of new particles, as previously reported.[42] This color change occurs due to the ability of plant extract components to interact with metal ions and facilitate their conversion into CuO-Se BNPs.[38] Similar findings were demonstrated by Tabrez et al,[60] who synthesized and characterized green CuO NPs using leaf extract. Zughaibi, together with others,[61] synthesized CuO NPs using leaf extract and assessed their antitumor effects on breast cancer,[62] studied the biological uses of *Pluchea indica* leaves to biosynthesize selenium-gold BNPs. Hashem et al[63] found that watermelon peel was used to biosynthesize selenium-silver BNPs. Their study involved a comprehensive process where the peel extract was combined with metal salts to facilitate the reduction and stabilization

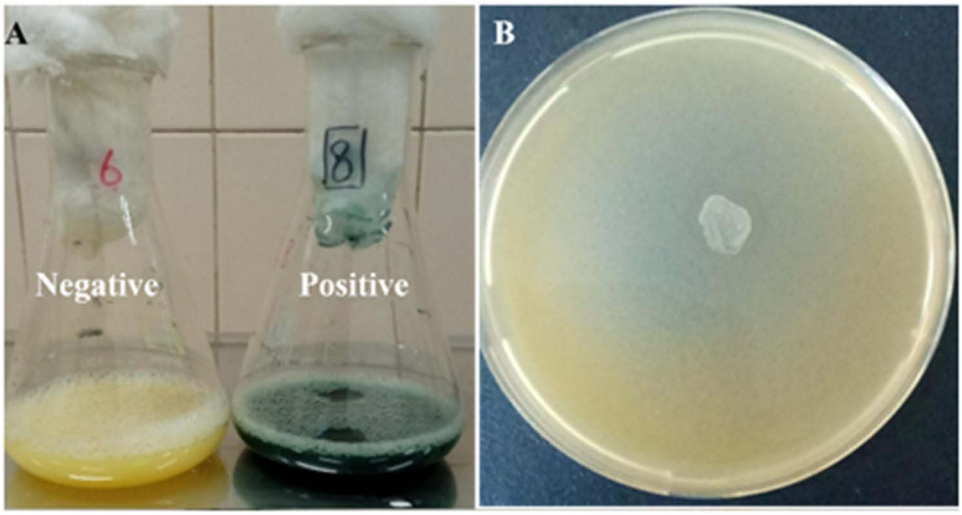

Figure 1 Representative qualitative production of some virulence factors by *P. aeruginosa* clinical isolates number 8. (**A**) The bluish green color indicating pyocyanin biosynthesis by isolate. (**B**) Clear zone associated with protein hydrolysis was the unblemished base for proteolytic activity.

https://doi.org/10.2147/IJN.S497494

Table 1 Different CuO-Se BNPs Anti-Pseudomonas Activity

Isolates*	Production of QS Associated Factors		Well Diffusion Assay			Broth Microdilution Assay			
			CRO	CuO-Se BNPs		CuO-Se BNPs Activity			
	PC	PT	IZD (mm)		PI (%)	MIC*	MBC	T	In vitro Effect
Ps_1	-ve	-ve	18.33±0.4	0±0	N/A	250±0.0	500	2	Bactericidal
Ps_2	+ve	-ve	23.33±0.4	0±0	N/A	250±0.0	500	2	
Ps_3	-ve	-ve	24.33±0.4	19.67±0	87	7.8±0.0	125	16	Bacteriostatic
Ps_4	+ve	-ve	16.67±0.4	21±0	87	7.8±0.0	125	16	
Ps_5	-ve	-ve	25.33±0.4	11.33±0	65	31.2±0.0	125	4	Bactericidal
Ps_6	-ve	+ve	22.33±0.4	16.33±0	64	31.2±0.0	250	8	Bacteriostatic
Ps_7	+ve	+ve	23.33±0.4	0±0	N/A	250±0.0	500	2	Bactericidal
Ps_8	+ve	-ve	15.67±0.4	20.33±0	87	15.6±0.0	250	16	Bacteriostatic
Ps_9	-ve	-ve	14.33±0.4	0±0	N/A	250±0.0	500	2	Bactericidal
Ps_{10}	+ve	+ve	21.67±0.4	0±0	N/A	250±0.0	500	2	
Ps_{11}	-ve	-ve	19±0	20.33±0	95	7.8±0.0	31.2	4	Bactericidal
Ps_{12}	-ve	+ve	18±0	0±0	N/A	250±0.0	500	2	
Ps_{13}	+ve	+ve	34±0.82	10±0	55	62.5±0.0	125	2	
Ps_{14}	-ve	-ve	27.33±0.9	16±0	48	15.6±0.0	125	8	Bacteriostatic
Ps_{15}	-ve	-ve	34±0.82	0±0	N/A	250±0.0	500	2	Bactericidal
Ps_{16}	-ve	+ve	26.33±0.4	0±0	N/A	250±0.0	500	2	
Ps_{17}	-ve	-ve	21.33±0.4	10±0	38	31.2±0.0	125	4	Bactericidal
Ps_{18}	-ve	+ve	24±0	20±0	95	15.6±0.0	125	8	Bacteriostatic
Ps_{19}	-ve	+ve	20±0	10±0	42	31.2±0.0	62.5	2	Bactericidal
Ps_{20}	+ve	-ve	21±0	0±0	N/A	250±0.0	500	2	
Ps_{21}	-ve	-ve	25.33±0.9	0±0	N/A	250±0.0	500	2	
Ps_{22}	-ve	-ve	25.67±0.4	15.67±0	61	15.6±0.0	125	8	Bacteriostatic
Ps_{23}	-ve	-ve	31±0	13.67±0	54	31.2±0.0	125	4	Bactericidal
Ps_{24}	-ve	-ve	18.33±0.4	12±0	39	31.2±0.0	125	4	

Notes: * Ps_1-Ps_{24}; *P. aeruginosa* clinical isolates (1–24). Results are expressed as mean value ± Standard Deviation (SD).
Abbreviations: QS, quorum sensing; PC, pyocyanin; PT, protease; CRO, ceftriaxone; IZD, inhibition zone diameter; PI, percent inhibition; MIC, minimum inhibitory concentration; MBC, minimum bactericidal concentration; T, tolerance; -ve, negative; +ve, positive; N/A, not applicable.

of the NPs. The resulting selenium-silver BNPs exhibited notable antimicrobial and antioxidant properties, which were evaluated using various in vitro assays.

Characterization of CuO-Se BNPs

UV-Vis Spectroscopy

UV-vis spectroscopy is a practical method for verifying the creation and stability of metal NPs in aqueous solutions. The effective synthesis of bimetallic NPs using leaf extract was confirmed by the presence of surface plasmon resonance

(SPR) bands in the UV-vis spectra of the NPs. The SPR band maximum of the NPs was observed at 330 nm (Figure 2). During the reaction, the hue gradually shifted from blue to dark green, and the concentration of leaf extract produced SPR.[64] According to Hashem et al, the produced B_2O_3-ZnO BNPs had a small and detectable UV-Vis of 370.0 nm.[65] The UV-vis spectra of selenium-silver BNPs showed a peak at 380 nm, with an optical density (OD) of 0.295 (diluted 30 times) as observed by Hashem et al.[63] Moreover, peel extract reduced metal ions into an Ag-ZnO nanoscale composite, as evidenced by the UV spectra of the Ag-ZnO nanocomposite peak at 345 nm.[66] Hasanin et al[67] displayed the UV-vis spectra of ZnO-CuO NPs and ZnO-CuO NPs/CSC, showing peaks at 326, 365, and 410 nm, which confirm the successful mycosynthesis of ZnO-CuO BNPs. Idris and Roy,[68] reported that the UV-vis spectrum of green synthesized Ag-Fe_2O_3 BNPs exhibited two absorption peaks: one at 290 nm and another at 350 nm. Other studies have found that the SPR band maxima of monometallic CuO NPs and MnO NPs are at 336 nm and 266 nm, respectively.[42] UV-vis spectroscopy was used to validate the production of SeNPs, and the results showed that a distinct peak developed at 263 nm when employing pumpkin seed extract.[69] Furthermore, the unique peak at 336 nm for CuO NPs indicates the characteristic surface plasmon resonance of the nano-sized particles, as demonstrated by the use of pumpkin seed.[60]

FTIR Spectroscopy

The FTIR spectra provide critical insights into the functional groups involved in the biosynthesis of CuO-Se BNPs. The FTIR spectrum of *L. siceraria* leaf extract (spectrum A, Figure 3) exhibits prominent peaks characteristic of various phytochemical constituents. A strong broad peak at 3309 cm^{-1} corresponding to O-H stretching vibrations, typically associated with phenolic and alcoholic groups present in bioactive compounds such as flavonoids and polyphenols.[70] A peak at 2923 cm^{-1} attributed to C-H stretching in aliphatic hydrocarbons.[71] A peak at 1605 cm^{-1} indicates C=C stretching vibrations in aromatic rings or C=O stretching in ketones and aldehydes.[72] A peak at 1019 cm^{-1} corresponds to C-O-C stretching vibrations of ethers.[72] The peaks presented at 508–431 cm^{-1} represents the vibrational modes of trace metals naturally present in the extract, potentially interacting during the synthesis process.[73] These functional groups act as reducing and capping agents, facilitating the biogenic synthesis of NPs.[74]

On another hand, the FTIR spectrum of CuO-Se BNPs (spectrum B, Figure 3) reveals significant shifts and the appearance of new peaks. The peak presented at 3278 cm^{-1} a noticeable decrease in the intensity of the O-H stretching vibration suggests the involvement of hydroxyl groups in the reduction of Cu^{2+} and Se^{4+} ions.[75] The appearance of new bands at 2312–1971 cm^{-1} may indicate the formation of metal-oxygen or metal-selenium bonds, consistent with Cu-O and Se-O interactions.[74] A shift in C=C or C=O vibrations observed at the band 1423 cm^{-1} reflects modifications in organic compounds, likely due to their interaction with the NPs surface.[76] The peaks observed at 524–447 cm^{-1} are characteristic of Cu-O and Se-O stretching vibrations, confirming the successful formation of CuO-Se BNPs.[77]

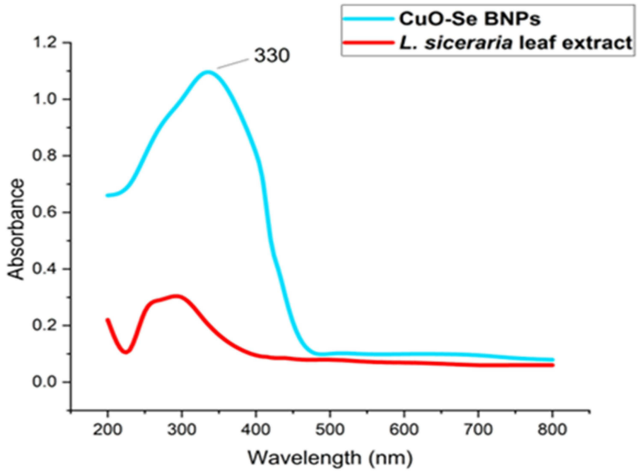

Figure 2 The UV-vis spectroscopy of CuO-Se BNPs and *L. siceraria* leaf extract.

https://doi.org/10.2147/IJN.S497494

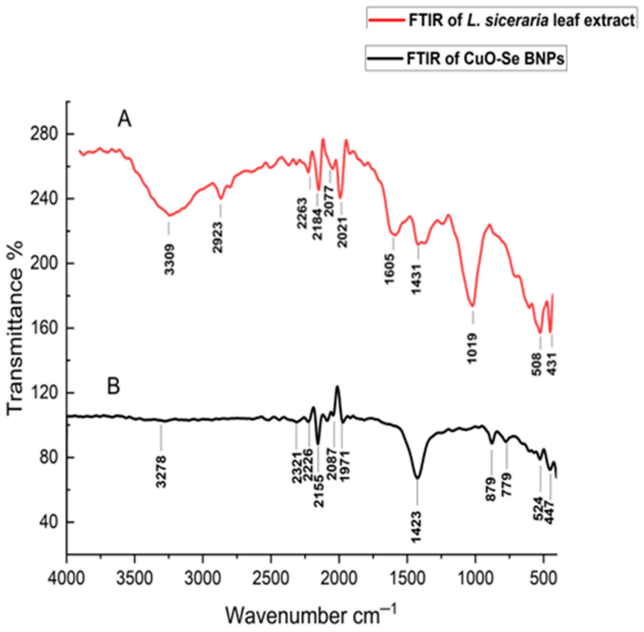

Figure 3 The FTIR analysis of *L. siceraria* (**A**) and CuO-Se BNPs (**B**).

Proposed Mechanism of Reduction and Stabilization

The phytochemicals in the *L. siceraria* leaf extract, particularly phenols, flavonoids, and hydroxylated compounds, play a dual role as reducing agents and stabilizers.[78] The O-H and C=O groups donate electrons, reducing Cu^{2+} and Se^{4+} ions to their respective metallic or oxide states. Simultaneously, these phytochemicals adsorb onto the NPs surface, providing a capping layer that prevents agglomeration and enhances stability.[77,79]

XRD Pattern of CuO-Se BNPs

XRD pattern of CuO-Se BNPs: The XRD pattern was utilized to analyze the crystalline structures of CuO-Se BNPs (Figure 4). Diffraction peaks corresponding to CuO were observed at 2θ = 32.5°, 35.7°, 38.9°, 48.8°, 62.1°, and 66.0°, which are attributed to the Miller indices planes of 110, 111, 202, 020, 113, and 311. These peaks correspond to a face-centered cubic structure, consistent with JCPDS-01-080-0076 for CuO NPs with a monoclinic phase. However, Tabrez et al[60] used the JCPDS reference JCPDS-05-0661, which corresponds to a monoclinic CuO structure, with diffraction peaks at similar 2θ values but with slight variations in the intensity and positions of the peaks. Both references are valid, but in this study, JCPDS-01-080-0076 was used for CuO identification. The XRD pattern of SeNPs revealed diffraction peaks at 2θ = 29.8°, 32.5°, 46.3°, 56.9°, and 66.0°, corresponding to the planes (100), (110), (111), (201), and (311). All the peaks were like JCPDS of SeNPs with a standard card like JCPDS File No. 06–0362. The lower intensities are due to the obstructive effect of the amorphous particles. These peaks, with lowered

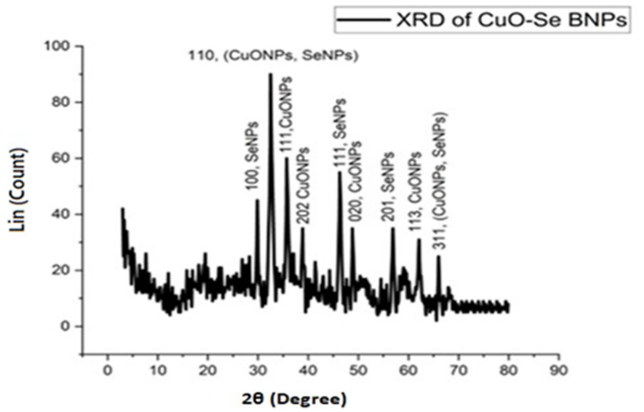

Figure 4 XRD of CuO-Se BNPs.

intensity and significant broadening, indicate the crystalline nature of SeNPs. Sarkar et al found the identical result.[80] The XRD of SeNPs produced by at plans (100), (110), (101), (111), and (102) revealed typical peaks with lowered intensity and significant widening. The broadening can be attributed to the presence of amorphous particles, which obstruct the sharper diffraction peaks typical of well-crystallized materials. Based on visual inspection, the sample contains a mix of both amorphous and crystalline phases, but the crystalline phases dominate. The amorphous phase likely influences the functional properties of the NPs by affecting their stability, surface reactivity, and potentially reducing their photocatalytic efficiency. The combination of CuO and Se in the bimetallic CuO-Se NPs did not result in significant structural distortions, but slight peak broadening was observed, possibly due to interactions between the two metals. However, there were no substantial shifts in the diffraction peaks that would indicate major structural distortions in the crystalline lattice. This suggests that the bimetallic nature does not drastically alter the crystalline structures of the individual components. These findings are consistent with the observations of Hashem et al,[81] who reported similar results for SeNPs synthesized using pomegranate peel extract, and Shahbaz et al,[69] who also noted no significant peak shifts in SeNPs. In summary, the combination of CuO and Se into CuO-Se BNPs retains the general crystalline structures of the monometallic components, with minor broadening in the XRD peaks, indicative of the formation of the BNPs. The crystallite size was calculated using the Scherrer equation,[82] yielding an average size of approximately 50 nm.

SEM and EDX Analyses

SEM and EDX investigations were used to examine the surface morphology of the produced CuO-Se BNPs (Figure 5). The SEM image (Figure 5A) demonstrates detailed surface morphology, highlighting a complex structure composed of aggregated particles and column-like or needle-like nanoforms. These formations suggest an organized nanoscale growth or crystallization process. The dense clusters visible in the image indicate partial crystallization, revealing fine structural

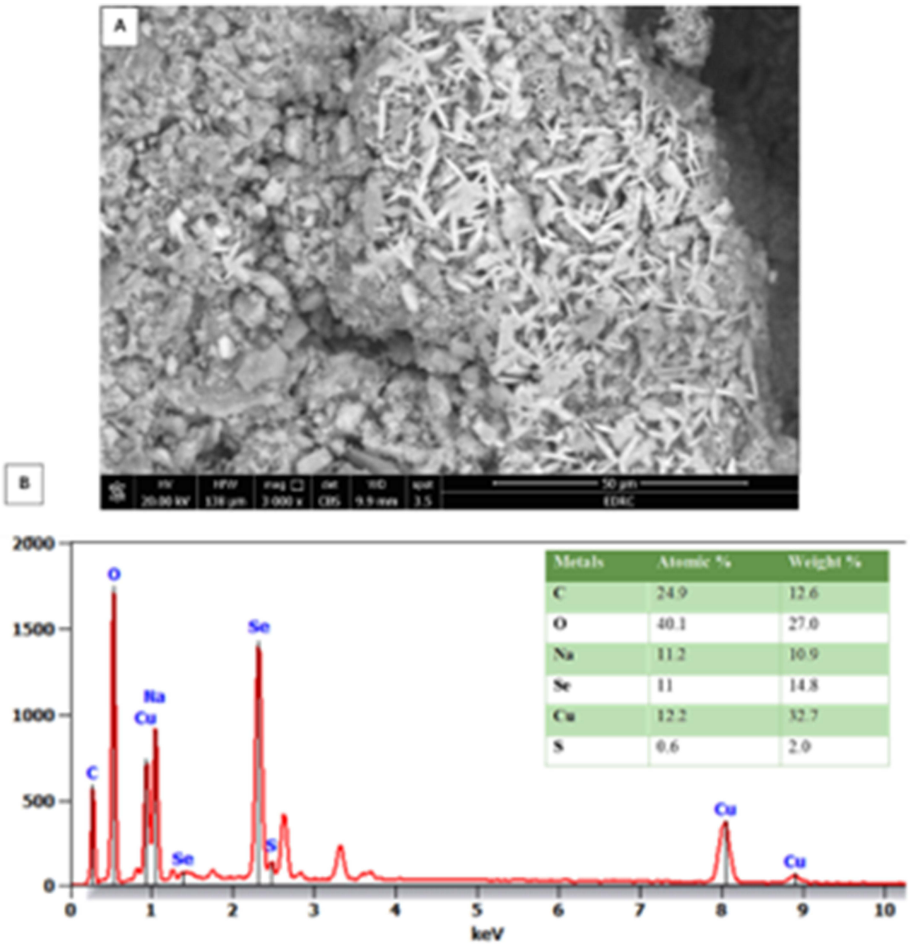

Figure 5 SEM (**A**) and EDX spectra and elemental composition of biosynthesized CuO-Se BNPs (**B**).

https://doi.org/10.2147/IJN.S497494

characteristics, while the needle-like shapes may represent metallic or nanocrystalline materials. The scale bar indicates 50 micrometers (μm), and the image was captured at a magnification of 3000× as annotated. The imaging parameters include an accelerating voltage (HV) of 20.00 kV, ensuring high contrast and resolution of intricate features, while the spot size of 3.5 enhances focus and minimizes noise. An area of the SEM picture was chosen for EDX analysis to verify the elemental composition of the NPs (Figure 5B). The findings showed that 32.7 weight percent Cu and 14.8 weight percent Se make up the CuO-Se BNPs. EDX provided further confirmation of the CuO-Se BNPs' crystallinity. Important information on the morphology and elemental composition of the produced CuO-Se BNPs is provided by the EDX and SEM studies. The inclusion of additional phytochemical components from the EDX spectrum that may result from the *L. siceraria* leaf extract acting as the capping agent is one benefit of green synthesis. This can be attributed to the high capping agent content in the reaction liquid, the copper grid, or other analytic additives.[83] CuO-Se BNPs may have had biomolecules covering their surface because of the presence of C, O, Na, and S. These elements correlate with functional groups such as hydroxyl (-OH), carboxyl (-COOH), and sulfate ($-SO_3^-$) groups, commonly found in phytochemicals like flavonoids, phenolic acids, terpenoids, and alkaloids. These biomolecules act as stabilizing agents, preventing agglomeration of the NPs.[74] Tomke and Rathod investigated the elemental makeup of a Fe_3O_4@ Chitosan–Ag NP nanocomposite using the EDX spectrum.[84] The elemental composition of the NPs showed 84.91% copper and 15.04% manganese, confirming the creation of Cu-Mn BNPs in accordance with Alafaleq et al's[42] description.

Phytochemicals play a crucial role in stabilizing NPs through the reduction and capping processes. For example, phenolic compounds (eg, flavonoids) contain hydroxyl groups that can bind to metal ions, creating a protective shell around the NPs.[22] This capping agent not only stabilizes the NPs but also influences their size and shape.

TEM and DLS Analysis

TEM examination was used to assess the size and surface morphology of the biosynthesized CuO-Se BNPs (Figure 6A). The TEM is a useful method that provides information on the shape, mean size, and dispersion of NPs. The biosynthesized CuO-Se BNPs were discovered to be spherical, with an average particle size of 30 nm and a size range of 5 to 50 nm. The particles also exhibited the shell of *L. siceraria*, indicating the aggregation of two or more particles. The effective creation of CuO-Se BNPs from *L. siceraria* leaf extract was proven by the chemical characterization performed using SEM, EDX, and TEM. The CuO-Se BNPs should be examined from a polycrystalline viewpoint, according to the SAED (Figure 6B). The created Ag NPs, Au NPs, and Ag–Au BNPs were formed in a variety of ways, including spherical and oval forms, according to TEM images provided by El-Batal et al.[85] DLS is an effective method for thoroughly examining the distribution and interactions of particles floating in liquids. The NPs in our work had an anisotropic form and good stability due to the employment of *L. siceraria* leaf extract as a reducing and capping agent. Furthermore, data from TEM and DLS were used to conduct a comparative analysis. The size determined by TEM refers to the physical diameter of the NPs themselves. The technique is highly accurate, but the size measurements are based on the direct image of individual particles.[86] DLS measures the hydrodynamic size of NPs, which includes not only the size of the particles themselves but also the layer of solvent or stabilizing agents (such as proteins or surfactants) that may surround the particles in a solution. This results in a larger size estimate compared to TEM. DLS measures the diffusion rate of particles in suspension, which is influenced by both the NPs' size and the surrounding medium.[87,88] Using the DLS method, the particle size distribution of the CuO-Se BNPs that were biosynthesized using *L. siceraria* leaf extract was determined. As can be seen in Figure 6C, the study showed that the average particle size was 79 nm. Because DLS size measurements evaluate the hydrodynamic radius of NPs in the presence of water molecules (solvent shell), which results in bigger particle sizes of the capped NPs, they often produce superior findings than TEM measurements.[89] However, TEM analysis allows one to determine the true size of the material's particles without considering the solvent layer's existence. This "hydration shell" effect can vary depending on the type of NPs and the solution conditions (eg, solvent type, concentration, etc). The most current DLS data showed that all the synthesized NPs had a PDI of 0.27 and were evenly distributed. On the other hand, polydispersity particle diffusion is expected to occur at values higher than 0.4.[90] According to the available data, the biosynthesized CuO-Se BNPs had a moderate mono-size dispersion.

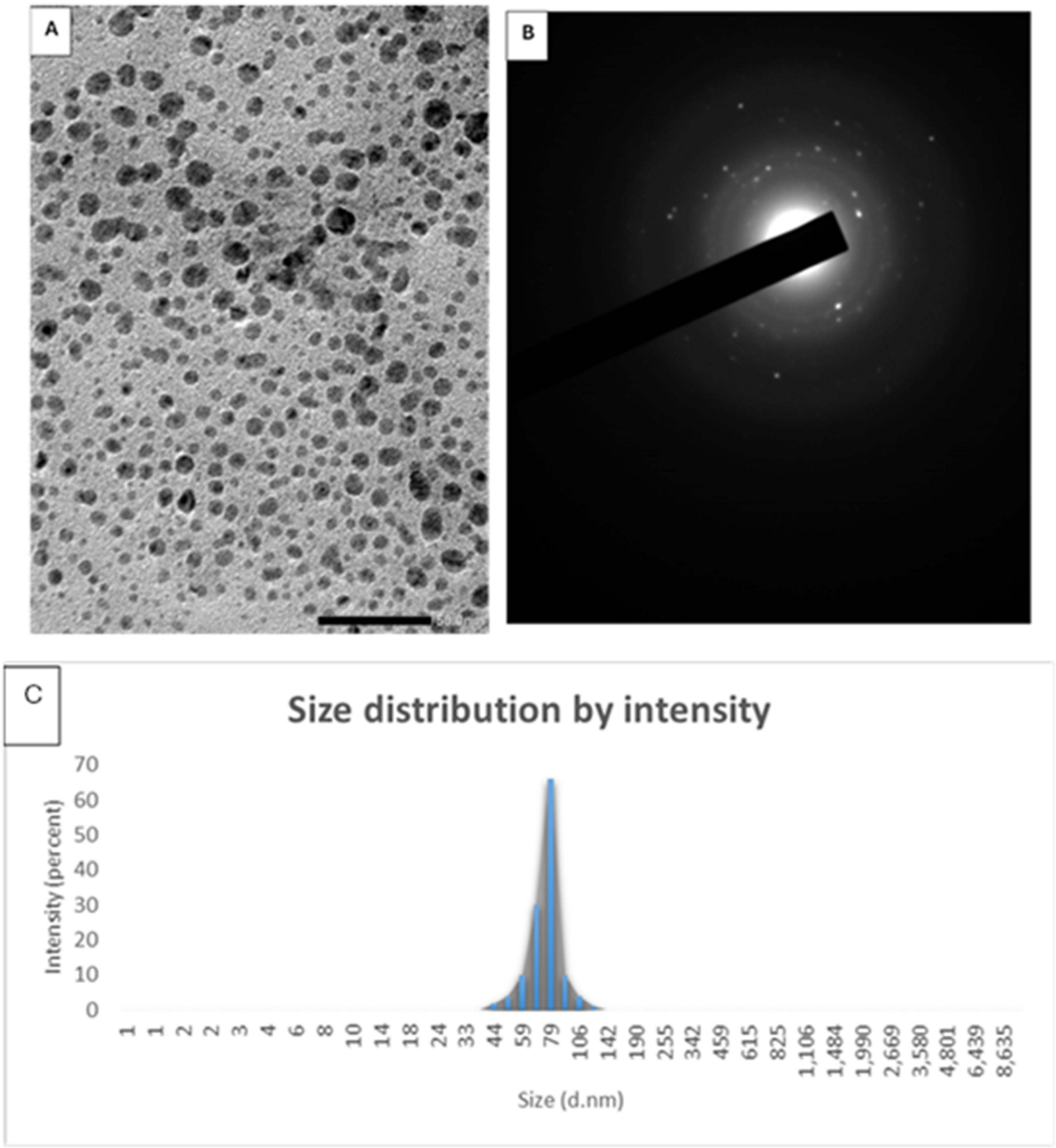

Figure 6 (**A**) TEM analysis showing different sizes of CuO-Se BNPs (Bar size 50.0 nm), (**B**) SEAD pattern of CuO-Se BNPs, and (**C**) DLS analysis.

Planktonic Bacterial Growth Inhibitory Effect

At the side of antimicrobial activity, a remarkable anti-pseudomonas initial activity, in comparing with the ceftriaxone standard positive control, of CuO-Se BNPs at 2000 µg/mL was noticeable (Figure 7). The CuO-Se BNPs efficiently inhibited the bacterial growth around the well at a zone diameter in the range of 10–21 mm (Table 1). As well, the reported percent inhibition of CuO-Se BNPs against the susceptible isolates was in the range of 38–95%. The study conducted by[91] recorded various IZD by agar diffusion assay and demonstrated an enhanced higher CuO-Ag BNPs antibacterial effectiveness than the Cu NPs or Ag NPs against the Gram-negative bacterium, *Escherichia coli*. As well,

https://doi.org/10.2147/IJN.S497494

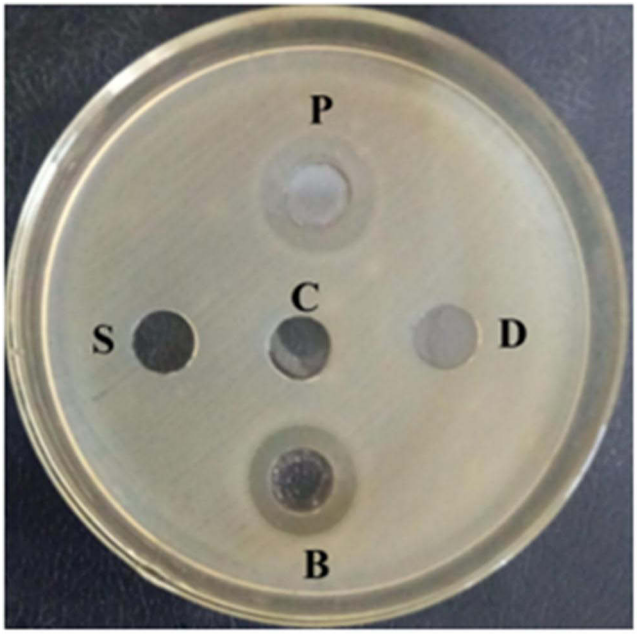

Figure 7 Representative agar well diffusion assay of CuO-Se BNPs illustrating the growth inhibition activity against *P. aeruginosa* clinical isolate (Ps_{18}). Wells P; ceftriaxone positive control (50 μg/mL), S; sodium selenite (100 μg/mL), C; copper acetate (100 μg/mL), D; DMSO negative control (8%), and B; CuO-Se BNPs (2000 μg/mL).

the research carried out by[92] the agar well diffusion assay demonstrated the preeminent antibacterial potential of the Ag-Au BNPs against *P. aeruginosa* in comparing with each monometallic NPs activity. However, the variable IZD obtained from each agar diffusion assay illustrated the variation in the BNPs activity against the tested bacterial isolates. Also, the acceptable percent inhibition (Table 1) clarifies the enhanced CuO-Se BNPs activity that could attributed to the wide range of bimetallic targets.

Mechanism of action of CuO-Se BNPs may be attributed to electrostatic interaction which cause cell membrane damage, disruption of proteins and enzymes, ROS generation and oxidative stress, protein binding which leads to homeostasis disturbance (electron transport chain disruption), signal transduction inhibition and genotoxicity.[93,94] Also, the efficacy may be attributed to roughness of external surface of NPs which cause damaging the cell wall; these lead to penetrate NPs to plasma membrane and causing toxicity to bacteria.[95]

Furthermore, the broth microdilution assay (Figure 8) illustrated the quantitative ability of the CuO-Se BNPs to thwart the growth of the tested *P. aeruginosa* isolates. The recorded MICs and MBCs were in the range of 7.8–250 μg/

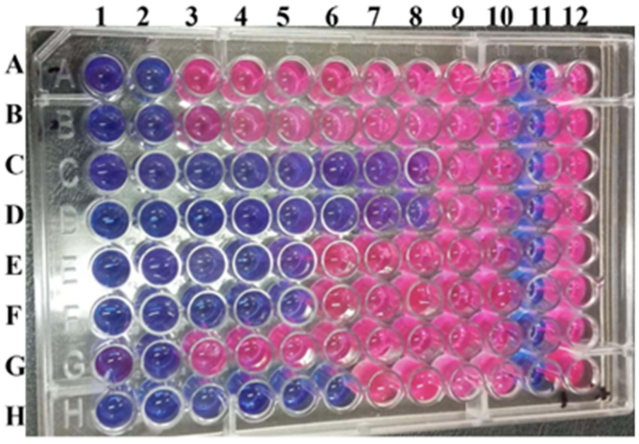

Figure 8 Broth microdilution assay using resazurin dye showing variable inhibitory effects of CuO-Se BNPs against *P. aeruginosa* clinical isolates Ps_1-Ps_8 in row A-D, respectively at a range of 500–3.906 μg/mL (columns 1–10, respectively). The negative and positive control tests are represented by columns 11 and 12, respectively.

mL and 31.2–500 µg/mL, respectively. Additionally, the calculated tolerance level, which is represented by the MBC/MIC ratio (Table 1), illustrates the variable bactericidal and bacteriostatic effect of our NPs against the tested bacterial isolates depending on the value of tolerance level of <4 (bactericidal) or ≥4 (bacteriostatic). Additionally, the calculated tolerance level illustrates the variable bactericidal/bacteriostatic effect of our NPs against the tested bacterial isolates (Table 1). In a related study, a comparable MIC and MBC (240 µg/mL each) of the biosynthesized Ag-Cu BNPs was recorded against *P. aeruginosa* with tolerance level equal to one indicating its bactericidal activity against their tested strains.[96] Likewise, the study conducted by[97] recorded up to six times antibacterial activity for Cu and Ag NPs mixture higher than the totality of each separated monometallic NPs antibacterial effects against *P. aeruginosa*. Also, Cu-Ag BNPs synergistic effect on *P. aeruginosa* viability was noticeable with elevated bactericidal activity.[98] Also, complete eradication of *P. aeruginosa* was explored when exposed to Cu-Pd BNPs at 6 µg/mL, the effect that not achieved by separate exposure to Cu NPs or Pd NPs even at a concentration of 24 µg/mL.[99] Our results elucidate the BNPs low MIC and subsequent high activity. The improved BNPs antibacterial efficiency could be explained by the variation in the reactive edges and various irregular particle shapes with multiple binding sites of the combined NPs on microbial cell surface. Consequently, the CuO-Se BNPs superior hopeful efficacy could indicate their possible future antibacterial applicability.

Anti-Pyocyanin Effect

The bluish green pyocyanin, a phenazine pigment directly controlled by QS, is hallmark 2^{ry} metabolite of *P. aeruginosa* causing severe toxicity to host cells. In our study, the estimated CuO-Se BNPs effect on *P. aeruginosa* pyocyanin exotoxin has proven its interference with this pigment production in all the tested pyocyanin producing isolates (Figure 9). The anti-exotoxin activity was exhibited as pyocyanin inhibitory percentage with a relatively wide range of 4.35–63.21% (Table 2). In related research, inhibition of *P. aeruginosa* pyocyanin virulent component was concentration dependent where 128 µg/mL Au NPs exhibited 66.15% as a highest observed pyocyanin inhibition percentage.[100] Also, the discovered inhibition of *P. aeruginosa* pyocyanin production by 1024 µg/mL ZnO NPs or Au NPs was dramatically at 82.15% and 71.07%, respectively.[101] Likewise, biogenic ZnO NPs reduced the pyocyanin production by *P. aeruginosa* clinical isolates in concentration dependent manner. At a dose of 300 µg/mL, the pyocyanin reduction was in a range of 58.5%–67.7%. A lower reduction rate of 45.08% and 54.3% were observed with ZnO NPs concentration of 200 µg/mL and 100 µg/mL, respectively.[102] Additionally, investigation of *P. aeruginosa* clinical isolates pyocyanin production in presence of Ag NPs clarified the significant reduction in pyocyanin production with increased NPs concentration.[103] Moreover, similar results were reported by[104] study of gold NPs effect on *P. aeruginosa* PAO1 pyocyanin production. The gold NPs, at concentrations of 0.256, 0.128, and 0.032 mg/mL, decreased the pyocyanin production by 87.7, 81.9, and 79.4%, respectively. The anti-pyocyanin activity of different NPs suggesting their possible suppressive effect on the genetic determinants controlling *P. aeruginosa* pyocyanin pigment biosynthesis and consequently phenotypically inhibitory effect. However, the decreased *P. aeruginosa* pyocyanin biosynthesis by different NPs could be respected as an

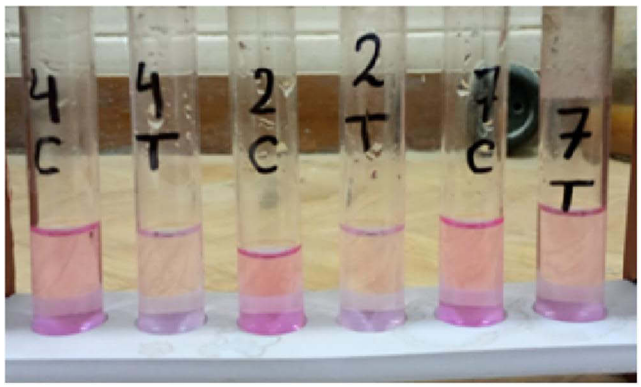

Figure 9 Representative anti-pyocyanin activity of CuO-Se BNPs. 2, 4, and 7 represent the isolate number, (C) was the control, and (T) was the test.

 https://doi.org/10.2147/IJN.S497494

Table 2 Anti-Virulence Activities of CuO-Se BNPs

Isolates*	Inhibitory Effect of 0.5 MIC CuO-Se BNPs (%)				Isolates	Inhibitory Effect of 0.5 MIC CuO-Se BNPs (%)			
	PC	PT	PVD	BF		PC	PT	PVD	BF
Ps_1	N/A	N/A	4.01	3.67±0.01	Ps_{13}	44.82	10.15	17.47	8.86±0.03
Ps_2	10.35	N/A	0.24	4.84±0.03	Ps_{14}	N/A	N/A	73.70	34.27±1.42
Ps_3	N/A	N/A	10.27	35.34±0.07	Ps_{15}	N/A	N/A	65.41	20.5±0.54
Ps_4	63.22	N/A	52.21	N/A	Ps_{16}	N/A	4.97	83.41	6.76±0.03
Ps_5	N/A	N/A	64.28	16.65±0.09	Ps_{17}	N/A	N/A	48.40	0.21±0
Ps_6	N/A	12.6	33.61	35.22±0	Ps_{18}	N/A	5.44	24.62	60.41±1.04
Ps_7	21.42	5.96	10.93	N/A	Ps_{19}	N/A	5.05	14.92	6.5±0.1
Ps_8	22.95	N/A	18.45	27.38±0.34	Ps_{20}	4.36	N/A	−1.22	11.68±0.59
Ps_9	N/A	N/A	−4.32	1.18±0.04	Ps_{21}	N/A	N/A	9.14	DIV/0!
Ps_{10}	23.56	6.33	24.01	1.76±0.06	Ps_{22}	N/A	N/A	2.77	22.14±0.76
Ps_{11}	N/A	N/A	−1.11	54.17±1.8	Ps_{23}	N/A	N/A	29.65	1.52±0.03
Ps_{12}	N/A	10.86	24.86	18.8±0.33	Ps_{24}	N/A	N/A	−2.66	36.22±0.33

Notes: * Ps_1-Ps_{24}; *P. aeruginosa* clinical isolates (1–24).
Abbreviations: PC, pyocyanin; PT, protease; PVD, pyoverdine; BF, biofilm formation; N/A, not applicable.

effective anti-virulent that diminish its host tissue colonization and pathogenesis. Importantly, biogenic NPs could represent an alternative ecofriendly and cost-effective pyocyanin inhibiting strategy that helps in controlling *P. aeruginosa* infection without selection for resistant strains.

Conversely, the study by[105] reported that pyocyanin pigment production by *P. aeruginosa* was increased when exposed to different concentration of Au NPs. Also, the study conducted by[106] recorded variable *P. aeruginosa* pyocyanin production in presence of different ZnO NPs concentrations. Pyocyanin suppressed production, by about 90%, was noticeable with 500 µg/mL ZnO NPs concentration, while the induced pyocyanin biosynthesis was observed at 7.31 µg/mL. The intensified biosynthesis of pyocyanin could represent a reflex protective mechanism associated with overexpression of virulent determinant encoding the produced pigment upon exposure to NPs at subinhibitory concentration. Hence, careful adjustment of the applied NPs concentration is critical to avoid the undesirable overproduction of pyocyanin at the exposure to sub-inhibitory concentrations.

Total Protease Inhibitory Effect

P. aeruginosa protease enzyme hydrolyzes the infected host tissue protein facilitating its invasion to underline tissue and pathogenicity progression. In our present study, the calculated inhibitory percentage of *P. aeruginosa* total protease activity caused by the biosynthesized CuO-Se BNPs clarify its anti-proteolytic activity. The obtained inhibition percentage of protease activity was recognized at a range of 4.96–12.59% (Table 2). Correspondingly, the suspension containing 15 µg/mL of biosynthesized Ag NPs was able to efficiently block 47.3% of *P. aeruginosa* proteolytic activity.[107] Also, *P. aeruginosa* clinical isolates biosynthesized decreased protease concentration by 24.1–39.3% when treated with 300 µg/mL biogenic ZnO NPs. However, at a lower ZnO NPs concentration (200 µg/mL), protease biosynthesis decreased at a range of 11.2–30.3%.[102] In a related study, exposure of *P. aeruginosa* to selective pressures caused by levofloxacin could resulted in the development of strains with extracellular protease-deficient property.[55] Similarly, the 110 µg/mL of vitexin, a polyphenolic flavone, caused moderate weakening of *P. aeruginosa* protease biosynthesis. Also, a maximum vitexin synergistic protease inhibitory interaction was observed in combination with 2.5 µg/mL gentamicin.[108] Furthermore,[109] observations clarified the in vitro anti-inflammatory effect associated with

P. aeruginosa protease enzyme inhibitors. These findings illustrate the possible quorum quenching properties of NPs through their interference with bacterial protease enzyme production with consequent anti-inflammatory effect.

Anti-Siderophore Production Activity

Pyoverdine biosynthesis is controlled via QS and stimulates *P. aeruginosa* growth with subsequent promotion of its pathogenicity. In the present study, our results illustrated the different levels of pyoverdine production that was relatively in accordance with[110] study in which 70% of the tested *P. aeruginosa* isolates were characterized by heterogenous ability to produce pyoverdine. Also, the variable quantitative effect of the CuO-Se BNPs on *P. aeruginosa* pyoverdine siderophore production was obvious. The results illustrated the diminishable effect of CuO-Se BNPs on the pyoverdine production at a range 0.24–83.41% in 20/24 (83.3%) of the tested *P. aeruginosa* clinical isolates (Table 2). Our results were relatively consistent with the previous findings observed by[100] who recorded pyoverdine disarming in *P. aeruginosa* treated with Au NPs in dose dependent manner and the greatest inhibition (95.07%) was recorded with 128 µg/mL Au NPs. As well, treatment with 2 µg/mL Ag NPs achieved 97.40% inhibition in *P. aeruginosa* pyoverdine secretion. This effect was associated with down-regulation of virulent genes associated with pyoverdine production.[111] Additionally,[101] study recorded concentration dependent inhibitory activity of ZnO NPs or Au NPs on *P. aeruginosa* pyoverdine production. The maximum inhibition percentage, 85.24% and 55.1%, was observed with 1024 µg/mL ZnO NPs and Au NPs, respectively. Also, the research carried out by[112] reported a tellurium nanorods reduction of pyoverdine biosynthesis in a dose-dependent way without affecting the planktonic growth of the exposed *P. aeruginosa*. On the other hand, *P. aeruginosa* exposure to vitexin (110 µg/mL) resulted in moderate reduction of pyoverdine. Furthermore, the research conducted by[113] observed reduced *P. aeruginosa* pathogenicity through only direct disruption pyoverdine function. The combination of direct pyoverdine toxicity as well as its iron scavenging activity and promotion of multiple virulence determinant expression makes the pyoverdine essential for *P. aeruginosa* pathogenesis. Accordingly, in *P. aeruginosa*, pyoverdine is a key virulent factor regulated by QS and interfering with cellular functions. The development of an effective alternative antimicrobial agent with the ability to combat *P. aeruginosa* production of pyoverdine may help in diminishing its virulence character via lowering the cellular iron uptake.[114]

Conversely, 4/24 (16.7%) of our tested *P. aeruginosa* clinical isolates showed a slight increase (1.1–4.3%) in pyoverdine biosynthesis after treatment with 0.5 MIC Cu-Ag NPs (Table 2). In a related study conducted by[115] exposure of *P. aeruginosa* to sub-MIC of the colloidal Ag NPs formulation (Silversol®) resulted in 1.5-fold enhancement in pyoverdine biosynthesis and upregulation of one pyoverdine regulating gene. More pyoverdine siderophore production in Ag NPs exposed bacterial cells could be resulted from the NPs iron-limitation effect. Hence, our results speculated the NPs iron-homeostasis disturbing activity in the tested *P. aeruginosa* isolates.

Biofilm Inhibitory Activity

The quantitative CV assay demonstrated the effective inhibitory outcome of CuO-Se BNPs, at 0.5 MIC, on each tested biofilm-forming *P. aeruginosa* isolate. The data revealed an inhibitory effect in the CuO-Se BNPs-treated cells in the form of reduced percentage of the biofilm growth form at the range of 0.21–60.72% (Table 2). Similarly, investigation of the Ag-Cu BNPs impact on *P. aeruginosa* biofilm formation using sub-inhibitory concentration revealed dose-dependent biofilm inhibitory effect. The findings illustrated a full inhibition of *P. aeruginosa* biofilm formation by 240 µg/mL of the biosynthesized NPs.[96] Also, the biogenic Ag-Au BNPs (100 µg/mL) showed about 19% inhibitory effect on *P. aeruginosa* biofilm formation.[116] While the biofilm growth form delays the antimicrobial penetration with consequent treatment failure, our results clarified the probable consideration of the tiny sized BNPs as antibiofilm strategy due to its possible high ability to cross the biofilm matrix with subsequent microbial cell destruction and prevention of biofilm formation.

Cytotoxicity of Biosynthesized CuO-Se BNPs

Biosafety of new compounds towards normal cell lines is a crucial aspect of drug development. Before a new compound can be considered for clinical trials, it must be tested for its potential toxicity to normal cells. This involves evaluating the compound's effects on cell viability, growth, and function using in vitro models of normal cell lines. Specifically, the

physicochemical properties of biogenic NPs could be customized via surface functionalization to improve their biocompatibility and interactive potentials against cancer cells. The bioengineering process for NPs synthesis is eco-friendly, cost-effective, and simple. The bioengineered NPs have a significant attention because of their unique biological and physicochemical properties that are useful as an innovative and alternative therapy that overcome the side effects and high costs of traditional cancer therapy.[27–29]

In the current study, biosafety of biosynthesized CuO-Se BNPs was checked toward Wi-39 normal cell line at different concentrations as shown in Figure 10A. Results revealed that, IC50 of biosynthesized CuO-Se BNPs against Wi-38 cell line was 267.2 µg/mL. Typically, if the IC50 is equal to or more than 90 µg/mL, the substance is categorized as non-cytotoxic.[117] Consequently, the CuO-Se BNPs are deemed to be safe for use. Therefore, safe concentrations and maximal non-toxic concentrations of CuO-Se BNPs were determined for anticancer activity.

Bimetallic NPs, particularly those composed of metals like gold, silver, copper, and selenium, have shown promising anticancer activity. These NPs can exhibit enhanced properties compared to their single-metal counterparts, including improved biocompatibility, targeted delivery, and enhanced therapeutic efficacy. In this study, biosynthesized CuO-Se BNPs were assessed for anticancer activity toward MCF-7 and Hep-G2 cancerous cell lines as illustrated in Figure 10B. Results show that biosynthesized CuO-Se BNPs exhibited promising anticancer activity against MCF-7 and Hep-G2, where IC50 were 31.1 and 83.4 µg/mL, respectively. To confirm the safety of the biosynthesized CuO-Se BNPs, the selectivity index (SI) was performed, where results showed that SI toward MCF-7 and Hep-G2 were 8.59 and 3.2, respectively. The biosynthesized CuO-Se BNPs SI values greater than two confirmed its acceptable selectivity toward both cancerous cell lines.

One key mechanism involves the induction of apoptosis, or programmed cell death, in cancer cells. CuO-Se BNPs can disrupt mitochondrial membrane potential, leading to the release of cytochrome c and the activation of caspase

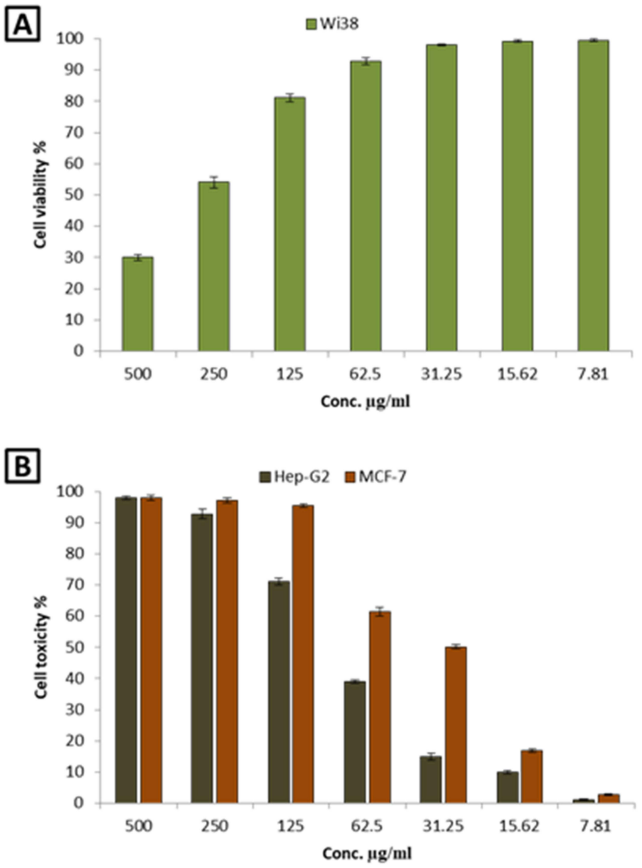

Figure 10 Cytotoxicity of CuO-Se BNPs toward the normal cell lines of Wi-38 (**A**) and the cancer cell lines of Hep-G2 and MCF-7 (**B**).

cascades, ultimately triggering the apoptotic cascade. Additionally, these NPs can generate reactive oxygen species (ROS) within cancer cells, inducing oxidative stress and damaging cellular components, leading to cell death.[118]

Furthermore, CuO-Se BNPs can interfere with cell cycle progression, preventing cancer cells from replicating and dividing uncontrollably. These NPs can also disrupt specific signaling pathways involved in cancer cell growth and survival, leading to their inhibition. CuO-Se BNPs can also act as drug carriers, delivering chemotherapeutic agents directly to tumor sites, improving drug efficacy and reducing side effects.[119,120] These NPs have also shown anti-angiogenic activity, inhibiting the formation of new blood vessels that supply nutrients to tumors, thereby starving them and hindering their growth.

Conclusions

This study demonstrated a successful synthesis of CuO-Se BNPs using an environmentally friendly, green synthesis approach employing *L. siceraria* leaf extract as a reducing and stabilizing agent. Characterization techniques confirmed the formation of core-shell CuO-Se BNPs with a particle size of approximately 50 nm, exhibiting a smooth, spindle-shaped morphology. The synthesized CuO-Se BNPs demonstrated significant antimicrobial activity against multi-drug resistant *P. aeruginosa*. Notably, they exhibited quorum-quenching properties, inhibiting the production of the quorum sensing molecule AHL, thereby reducing bacterial virulence. Additionally, the NPs suppressed the production of other virulence factors, including pyocyanin, proteases, and pyoverdine. Furthermore, the CuO-Se BNPs exhibited promising anticancer activity against MCF-7 and Hep-G2 cell lines at non-toxic concentrations. These findings suggest that CuO-Se BNPs have the potential to serve as a novel therapeutic agent for both bacterial infections and cancer, offering a sustainable and effective alternative to conventional treatments. Nevertheless, significant studies should be conducted to certify their stability and potentiality for large-scale production.

Data Sharing Statement

The datasets used and/or analyzed during the current study available from the corresponding author (Dr Amr Hashem) on reasonable request.

Acknowledgments

The authors really acknowledge the Faculty of Pharmacy and Faculty of Science, Al-Azhar University, Cairo, Egypt for offering the basic research facilities. This work was funded by the Researchers Supporting Project number (RSPD2025R725), King Saud University, Riyadh, Saudi Arabia. The authors also extend all their respect to Zarqa university-Jordan for partial funding of this research.

Author Contributions

All authors made a significant contribution to all parts in the work reported, whether that is in the study conception and design, data acquisition, analysis, and interpretation, or in all these areas; took part in drafting, revising or critically reviewing the article; gave final approval of the version to be published; have agreed on the journal to which the article has been submitted; and agree to be accountable for all aspects of the work.

Disclosure

The authors declare no competing interests.

References

1. Elfadadny A, Ragab RF, AlHarbi M, Badshah F, Ibáñez-Arancibia E. Antimicrobial resistance of Pseudomonas aeruginosa: navigating clinical impacts, current resistance trends, and innovations in breaking therapies. *Front Microbiol*. 2024;15:1374466. doi:10.3389/fmicb.2024.1374466
2. Ramatla T, Mokgokong P, Lekota K, Thekisoe O. Antimicrobial resistance profiles of Pseudomonas aeruginosa, Escherichia coli and Klebsiella pneumoniae strains isolated from broiler chickens. *Food Microbiol*. 2024;120:104476. doi:10.1016/j.fm.2024.104476
3. Liao C, Huang X, Wang Q, Yao D, Lu W. Virulence Factors of Pseudomonas Aeruginosa and Antivirulence Strategies to Combat Its Drug Resistance. *Front Cell Infect Microbiol*. 2022;12:926758. doi:10.3389/fcimb.2022.926758

4. Hibbert TM, Whiteley M, Renshaw SA, Neill DR, Fothergill JL. Critical analysis in the advancement of cell-based assays for botulinum neurotoxin. *Crit Rev Microbiol*. 2023;49(1):1–16. doi:10.1080/1040841X.2022.2035315
5. Muñoz-Cazalla A, Martínez JL, Laborda P. Crosstalk between Pseudomonas aeruginosa antibiotic resistance and virulence mediated by phenylethylamine. *Microb Biotechnol*. 2023;16(7):1492–1504. doi:10.1111/1751-7915.14252
6. Kolling D, Haupenthal J, Hirsch AKH, Koehnke J. Facile Production of the Pseudomonas aeruginosa Virulence Factor LasB in Escherichia coli for Structure-Based Drug Design. *Chembiochem*. 2023;24:e202300185.
7. Sathe N, Beech P, Croft L, Suphioglu C, Kapat A, Athan E. Pseudomonas aeruginosa: infections and novel approaches to treatment "Knowing the enemy" the threat of Pseudomonas aeruginosa and exploring novel approaches to treatment. *Infectious Medicine*. 2023;2(3):178–194. doi:10.1016/j.imj.2023.05.003
8. Ihssane B, Fatima E, Aboubakr K, Timinouni M, Kaotar N. New alternative therapeutic strategies against Pseudomonas aeruginosa, an opportunistic multi-resistant pathogen with a myriad of virulence factors. *J Infect Developing Countries*. 2023;17:891–904.
9. Albalawi MA, Abdelaziz AM, Attia MS, Saied E, Elganzory HH, Hashem AH. Mycosynthesis of Silica Nanoparticles Using Aspergillus Niger: control of Alternaria solani Causing Early Blight Disease, Induction of Innate Immunity and Reducing of Oxidative Stress in Eggplant. *Antioxidants*. 2022;11(12):2323. doi:10.3390/antiox11122323
10. Hasanin M, Hashem AH, Lashin I, Hassan SAM. In vitro improvement and rooting of banana plantlets using antifungal nanocomposite based on myco-synthesized copper oxide nanoparticles and starch. *Biomass Convers Biorefin*. 2023;13:8865–8875.
11. Prasad M, Lambe UP, Brar B, et al. Nanotherapeutics: an insight into healthcare and multi-dimensional applications in medical sector of the modern world. *Biomed Pharmacother*. 2018;97:1521–1537.
12. Gavas S, Quazi S, Karpiński TM. *Nanoparticles for Cancer Therapy: Current Progress and Challenge*. 2021;Vol. 16:173.
13. Ali OM, Hasanin MS, Suleiman WB, Helal EE-H, Hashem AH. Green biosynthesis of titanium dioxide quantum dots using watermelon peel waste: Antimicrobial, antioxidant, and anticancer activities. *Biomass Convers Biorefin*. 2024;14:6987–6998.
14. Karami MH, Abdouss M. Recent advances of carbon quantum dots in tumor imaging. *Nanomed J*. 2024;11:1.
15. Pandit C, Roy A, Ghotekar S, et al. Biological agents for synthesis of nanoparticles and their applications. *J King Saud Univ Sci*. 2022;34:101869.
16. Sharma G, Kumar A, Sharma S, Naushad M, Dwivedi RP, ALOthman ZA. Novel development of nanoparticles to bimetallic nanoparticles and their composites: a review. *J King Saud Univ Sci*. 2019;31:257–269.
17. Nyabadza A, McCarthy É, Makhesana M, Heidarinassab S, Plouze A, Vazquez M. *Science*. 2023;2023;103010.
18. Dlamini NG, Basson AK, Pullabhotla VSR. Wastewater treatment by a polymeric bioflocculant and iron nanoparticles synthesized from a bioflocculant. *Polymers*. 2023;4:1–24.
19. Khan S, Naushad M, Govarthanan M, Iqbal J, Alfadul SM. Emerging contaminants of high concern for the environment: current trends and future research. *Environ Res*. 2022;207:112609. doi:10.1016/j.envres.2021.112609
20. Hajam YA, Rai S, Kumar R, Bashir M. Phenolic compounds from medicinal herbs: their role in animal health and diseases–a new approach for sustainable welfare and development. *Plant Phenolics in Sustainable Agriculture*. 2020;2020:221–239.
21. Nyabadza A, McCarthy É, Makhesana M, et al. A review of physical, chemical and biological synthesis methods of bimetallic nanoparticles and applications in sensing, water treatment, biomedicine, catalysis and hydrogen storage. *Adv Colloid Interface Sci*. 2023;321:103010. doi:10.1016/j.cis.2023.103010
22. Ovais M, Khalil AT, Islam NU, Ahmad I, Shinwari ZK, Mukherjee S. Role of plant phytochemicals and microbial enzymes in biosynthesis of metallic nanoparticles. *Appl Microbiol Biotechnol*. 2018;102(16):6799–6814. doi:10.1007/s00253-018-9146-7
23. Berta L, Coman N-A, Rusu A, Tanase C. A review on plant-mediated synthesis of bimetallic nanoparticles, characterisation and their biological applications. *Materials*. 2021;14(24):7677. doi:10.3390/ma14247677
24. Lobo M. Biochemistry of vegetables: secondary metabolites in vegetables—terpenoids, phenolics, alkaloids, and sulfur-containing compounds. *Hounsome and v Processing*. 2018;26:47–82. doi:10.1002/9781119098935.ch3
25. Shahidi F, Varatharajan V, Oh WY, Peng HJFB. Phenolic compounds in agri-food by-products, their bioavailability and health effects. *Journal of Food Bioactives*. 2019;5:57–119. doi:10.31665/JFB.2019.5178
26. Minzanova ST, Mironov VF, Arkhipova DM, et al. Biological activity and pharmacological application of pectic polysaccharides: a review. *Polymers*. 2018;10:1407.
27. Majeed S, Saravanan M, Barabadi H, Mohanta YK, Mostafavi E. Bioengineering of green-synthesized TAT peptide-functionalized silver nanoparticles for apoptotic cell-death mediated therapy of breast adenocarcinoma. *Talanta*. 2023;253:124026.
28. Jounaki K, Nasiri A, Karami K, Jahani R. *Functionalized Nanomaterials for Cancer Research*. In: Barabadi H, Mostafavi E, Mustansar Hussain C, editor. Academic Press; 2024:219–260. doi:10.1016/B978-0-443-15518-5.00024-0
29. Nayak D, Chopra H, Chakrabartty I, Saravanan M, Barabadi H, Mohanta YK. *Bioengineered Nanomaterials for Wound Healing and Infection Control*. Barabadi H, Saravanan M, Mostafavi E, Vahidi H editor. Woodhead Publishing. 2023.:517–540. doi: 10.1016/B978-0-323-95376-4.00012-5
30. Jeevanandam J, Kiew SF. Green approaches for the synthesis of metal and metal oxide nanoparticles using microbial and plant extracts. *Nanoscale*. 2022;14:2534–2571.
31. Shah SMA, Akram M, Riaz M, Munir N, Rasool G. Cardioprotective Potential of Plant-Derived Molecules: a Scientific and Medicinal Approach. *Dose-Response*. 2019;17(2):1559325819852243. doi:10.1177/1559325819852243
32. Tripathi DK, Singh S, Singh S, Mishra S, Chauhan D. Micronutrients and their diverse role in agricultural crops: advances and future prospective. *Acta Physiol Plant*. 2015;37:1–14.
33. Al-Hakkani MFJSAS. Biogenic copper nanoparticles and their applications: A review. *SN Applied Sciences*. 2020;2:505. doi:10.1007/s42452-020-2279-1
34. Patil S. Biogenic nanoparticles: A comprehensive perspective in synthesis, characterization, application and its challenges. *Journal of Genetic Engineering and Biotechnology*. 2020;18:67. doi:10.1186/s43141-020-00081-3
35. Soni V, Raizada P, Singh P, Cuong HN, Rangabhashiyam S, Saini A. Sustainable and green trends in using plant extracts for the synthesis of biogenic metal nanoparticles toward environmental and pharmaceutical advances: a review. *Environmental Research*. 2021;202:111622. doi:10.1016/j.envres.2021.111622

36. Khurana A, Tekula S, Saifi MA, Venkatesh P. Therapeutic applications of selenium nanoparticles. Biomed Pharmacother. 2019;111:802–812.
37. Gao X, Li X, Mu J, et al. Preparation, physicochemical characterization, and anti-proliferation of selenium nanoparticles stabilized by Polyporus umbellatus polysaccharide. *International Journal of Biological Macromolecules*. 2020;152:605–615. doi:10.1016/j.ijbiomac.2020.02.199
38. Behera A, Mittu B, Padhi S, Patra N, Singh J. *Multifunctional Hybrid Nanomaterials for Sustainable Agri-Food and Ecosystems*. Elsevier; 2020:639–682.
39. Ashraf S, Liu Y, Wei H, et al. Bimetallic nanoalloy catalysts for green energy production: advances in synthesis routes and characterization techniques. *Small*. 2023;19:2303031. doi:10.1002/smll.202303031
40. Ozdal M, Gurkok S, Ozdal OG, Kurbanoglu EB. Enhancement of pyocyanin production by Pseudomonas aeruginosa via the addition of n-hexane as an oxygen vector. *Biocatal Agric Biotechnol*. 2019;22:101365.
41. Mohamed EA, Nawar AE, Hegazy EE. Insight into quorum sensing genes lasr and rhlr, their related virulence factors and antibiotic resistance pattern in Pseudomonas aeruginosa isolated from ocular infections. *Microbes and Infectious Diseases*. 2023;4:575–589.
42. Alafaleq NO, Zughaibi TA, Jabir NR, Khan AU, Khan MS, Tabrez SJN. Biogenic synthesis of Cu-Mn bimetallic nanoparticles using pumpkin seeds extract and their characterization and anticancer efficacy. *Nanomaterials*. 2023;13:1201.
43. Bhardwaj K, Singh AKJCEJA, Haak L. Significance of wastewater surveillance in detecting the prevalence of SARS-CoV-2 variants and other respiratory viruses in the community - A multi-site evaluation. *One Health (Amsterdam, Netherlands)*. 2023;16:100536. doi:10.1016/j.onehlt.2023.100536
44. Akbaribazm M, Khazaei F, Naseri L. Nasturtium Officinale L. hydroalcoholic extract improved oxymetholone-induced oxidative injury in mouse testis and sperm parameters. *Andrologia*. 2021;41:13294.
45. Salem SS, Badawy M. Green biosynthesis of selenium nanoparticles using Orange peel waste: characterization, antibacterial and antibiofilm activities against multidrug-resistant bacteria. *Life*. 2022;12:893.
46. Munazir M, Qureshi R, Arshad M, Gulfraz M. Antibacterial activity of root and fruit extracts of Leptadenia pyrotechnica (Asclepiadaceae) from Pakistan. *Pak J Bot*. 2012;44:1209–1213.
47. Elkady FM, Hashem AH, Salem SS, et al. Unveiling biological activities of biosynthesized starch/silver-selenium nanocomposite using Cladosporium cladosporioides CBS 174.62. *BMC Microbiol*. 2024;24(1):78. doi:10.1186/s12866-024-03228-1
48. Papa R, Imperlini E, Trecca M, et al. Virulence of Pseudomonas aeruginosa in Cystic Fibrosis: relationships between Normoxia and Anoxia Lifestyle. *Antibiotics*. 2024;13:1.
49. Tajani AS, Amiri Tehranizadeh Z, Fazly Bazzaz BS. Anti-quorum sensing and antibiofilm activity of coumarin derivatives against Pseudomonas aeruginosa PAO1: insights from in vitro and in silico studies. *Iran J Basic Med Sci*. 2023;26(4):445–452. doi:10.22038/IJBMS.2023.69016.15047
50. Naik P, Pandey S, Gagan S, Biswas S, Joseph J. Virulence factors in multidrug (MDR) and Pan-drug resistant (XDR) Pseudomonas aeruginosa: a cross-sectional study of isolates recovered from ocular infections in a high-incidence setting in southern India. *J Ophthalmic Inflamm Infect*. 2021;11(1):36. doi:10.1186/s12348-021-00268-w
51. Shehabeldine AM, Salem SS. Multifunctional silver nanoparticles based on chitosan: Antibacterial, antibiofilm, antifungal, antioxidant, and wound-healing activities. *Journal of Fungi*. 2022;8(6):612. doi:10.3390/jof8060612
52. Van de Loosdrecht A, Beelen R, Langenhuijsen M, Broekhoven MG, Langenhuijsen MM. A tetrazolium-based colorimetric MTT assay to quantitate human monocyte mediated cytotoxicity against leukemic cells from cell lines and patients with acute myeloid leukemia. *J Immunol Methods*. 1994;174(1–2):311–320. doi:10.1016/0022-1759(94)90034-5
53. Mudaliar SB, Bharath Prasad AS. A biomedical perspective of pyocyanin from Pseudomonas aeruginosa: its applications and challenges. *World J Microbiol Biotechnol*. 2024;40:90.
54. Shouman H, Said HS, Kenawy HI, Hassan R. Molecular and biological characterization of pyocyanin from clinical and environmental Pseudomonas aeruginosa. *Microb Cell Fact*. 2023;22(1):166. doi:10.1186/s12934-023-02169-0
55. Yang X, Zeng Q, Gou S, et al. Phenotypic heterogeneity unveils a negative correlation between antibiotic resistance and quorum sensing in Pseudomonas aeruginosa clinical isolates. *Front Microbiol*. 2024;15:1327675. doi:10.3389/fmicb.2024.1327675
56. Itto M, Asmae A, Mohammed T, Abdelhaq B. Virulence profiles of clinical and environmental Pseudomonas aeruginosa isolates from Central Morocco. *Afr J Microbiol Res*. 2016;10:473–480.
57. Hameed FA. Isolation of Pseudomonas Aeruginosa and Studying their Resistance and Pyocyanin Production. *Kirkuk J Sci*. 2024;19(1):24–31. doi:10.32894/kujss.2024.145615.1132
58. Galdino ACM, Branquinha MH, Santos ALS, Viganor L. *Pathophysiological Aspects of Proteases*. Chakraborti S, Dhalla NS, editors. Singapore: Springer Singapore; 2017:381–397. doi:10.1007/978-981-10-6141-7_16
59. Bhardwaj B, Singh P, Kumar A, Budhwar VJAPB. Eco-friendly greener synthesis of nanoparticles. *Advanced pharmaceutical bulletin*. 2020;10:566. doi:10.34172/apb.2020.067
60. Tabrez S, Khan AU, Mirza AA, et al. Biosynthesis of copper oxide nanoparticles and its therapeutic efficacy against colon cancer. *Nanotechnology Reviews*. 2022;11:1322–1331. doi:10.1515/ntrev-2022-0081
61. Zughaibi TA, Mirza AA, Suhail M, et al. Evaluation of anticancer potential of biogenic copper oxide nanoparticles (CuO NPs) against breast cancer. *Journal of Nanomaterials*. 2022;2022:5326355. doi:10.1155/2022/5326355
62. Aly Khalil AM, Saied E, Mekky AE, Saleh AM, Al Zoubi OM. Green biosynthesis of bimetallic selenium–gold nanoparticles using Pluchea indica leaves and their biological applications. *Front Bioeng Biotechnol*. 2024;11:1294170.
63. Hashem AH, El-Sayyad GS, Al-Askar AA, et al. Watermelon rind mediated biosynthesis of bimetallic selenium-silver nanoparticles: characterization, antimicrobial and anticancer activities. *Plants*. 2023;12:3288.
64. Kaur M, Singh J, Chauhan M, Kumar V, Singh KJOC. 2024;18:100571.
65. Hashem AH, Rizk SH, Abdel-Maksoud MA, Al-Qahtani WH, AbdElgawad H, El-Sayyad GSJR. Unveiling anticancer, antimicrobial, and antioxidant activities of novel synthesized bimetallic boron oxide–zinc oxide nanoparticles. *RSC advances*. 2023;13:20856–20867. doi:10.1039/D3RA03413E
66. Momeni A, Meshkatalsadat MH, Shahin BB, Mousavi YJHA. Photodegradation of methylene blue by phytosynthesized Ag–ZnO nanocomposites. Hybrid Advances. 2023;3:100050. doi:10.1016/j.hybadv.2023.100050

67. Hasanin MS, Hashem AH, Al-Askar AA, Haponiuk J. A novel nanocomposite based on mycosynthesized bimetallic zinc-copper oxide nanoparticles, nanocellulose and chitosan: characterization, antimicrobial and photocatalytic activities. *Electron J Biotechnol*. 2023;65:45–55.
68. Idris DS. Antioxidant and dye degradation activity of green synthesized silver-iron oxide (Ag-Fe2O3) bimetallic nanoparticles. *Nano-Struct Nano-Objects*. 2024;38:101142.
69. Shahbaz M, Akram A, Mehak A, et al. Evaluation of selenium nanoparticles in inducing disease resistance against spot blotch disease and promoting growth in wheat under biotic stress. *Plants*. 2023;12:761. doi:10.3390/plants12040761
70. Tafu NN, Jideani VA. Characterization of Novel Solid Dispersions of Moringa oleifera Leaf Powder Using Thermo-Analytical Techniques. *Processes*. 2021;9:2230.
71. Asemani M, Rabbani AR. Detailed FTIR spectroscopy characterization of crude oil extracted asphaltenes: curve resolve of overlapping bands. *J Petroleum Sci Eng*. 2020;185:106618.
72. Kumar AR, Selvaraj S, Devanathan J, et al. Multi-spectroscopic (FT-IR, FT-Raman, 1H NMR and 13C NMR) investigations on syringaldehyde. *J Mol Struct*. 2021;1229:129490.
73. Vignesh A, Amal TC, Kalaiyarasan J, Selvakumar S, Vasanth K. An effective bio-inspired synthesis of palladium nanoparticles using Crateva religiosa G. Forst. leaf extract: a multi-functional approach for environmental and biomedical applications. *Biomass Convers Biorefin*. 2023;2023:1–24. doi:10.1007/s13399-023-05031-w
74. Sidhu AK, Verma N, Kaushal P. Role of biogenic capping agents in the synthesis of metallic nanoparticles and evaluation of their therapeutic potential. *Front Biotechnol*. 2022;3:801620.
75. Ajitha B, Ashok Kumar Reddy Y, Sreedhara Reddy P. Biogenic nano-scale silver particles by Tephrosia purpurea leaf extract and their inborn antimicrobial activity. *Mater Sci Eng C*. 2015;49:373–381.
76. Khan M, Tareq F. Green synthesis and characterization of silver nanoparticles using Coriandrum sativum leaf extract. *J Eng Sci Technol*. 2018;13:158–166.
77. Chandran SP, Chaudhary M, Pasricha R, Ahmad A. Synthesis of Gold Nanotriangles and Silver Nanoparticles Using Aloevera Plant Extract. *Biotechnol Progress*. 2006;22:577–583.
78. El-Samahy LA, Tartor YH, Abdelkhalek A, Pet I, Ahmadi M, El-Nabtity SM. Ocimum basilicum and Lagenaria siceraria Loaded Lignin Nanoparticles as Versatile Antioxidant, Immune Modulatory, Anti-Efflux, and Antimicrobial Agents for Combating Multidrug-Resistant Bacteria and Fungi. *Antioxidants*. 2024;13:865.
79. Ahmad F, Ashraf N, Zhou R-B, Yin D-C, Yin D-C. Biological synthesis of metallic nanoparticles (MNPs) by plants and microbes: their cellular uptake, biocompatibility, and biomedical applications. *Appl Microbiol Biotechnol*. 2019;103(7):2913–2935. doi:10.1007/s00253-019-09675-5
80. Sarkar J, Chakraborty N, Dasgupta D, Acharya KJN. Green synthesized copper oxide nanoparticles ameliorate defence and antioxidant enzymes in Lens culinaris. *Nanomaterials*. 2020;10:312. doi:10.3390/nano10020312
81. Hashem AH, Saied E, Ali OM, Elkady FM. Pomegranate peel extract stabilized selenium nanoparticles synthesis: promising antimicrobial potential, antioxidant activity, biocompatibility, and hemocompatibility. *Appl Biochem*. 2023;195:5753–5776.
82. Muniz FTL, Miranda MR. The Scherrer equation and the dynamical theory of X-ray diffraction. *Foundations of Crystallography*. 2016;72:385–390. doi:10.1107/S205327331600365X
83. Sarwar N, Choi SH, Dastgeer G, et al. Synthesis of citrate-capped copper nanoparticles: a low temperature sintering approach for the fabrication of oxidation stable flexible conductive film. *Appl Surf Sci*. 2021;542:148609.
84. Tomke PD, Rathod VK. Facile fabrication of silver on magnetic nanocomposite (Fe3O4@Chitosan -AgNP nanocomposite) for catalytic reduction of anthropogenic pollutant and agricultural pathogens. *International Journal of Biological Macromolecules*. 2020;149:989–999. doi:10.1016/j.ijbiomac.2020.01.183
85. El-Batal AI, Abd Elkodous M, El-Sayyad GS, Al-Hazmi NE, Gobara M. Arabic polymer-stabilized and Gamma rays-assisted synthesis of bimetallic silver-gold nanoparticles: powerful antimicrobial and antibiofilm activities against pathogenic microbes isolated from diabetic foot patient. *Int J Biol Macromol*. 2020;165:169–186.
86. Modena MM, Rühle B, Burg TP, Wuttke SJAM. Nanoparticle characterization: what to measure?. *Advanced Materials*. 2019;31:1901556. doi:10.1002/adma.201901556
87. Jin L, Jarand CW, Brader ML. Angle-dependent effects in DLS measurements of polydisperse particles. *Meas SciTechnol*. 2022;33:045202.
88. Marucco A, Aldieri E, Leinardi R, Bergamaschi E, Riganti C, Fenoglio I. Applicability and Limitations in the Characterization of Poly-Dispersed Engineered Nanomaterials in Cell Media by Dynamic Light Scattering (DLS). *Material*. 2019;12(23):3833. doi:10.3390/ma12233833
89. Tareq SM. Detection and characterization of nanoparticles in the surface water: challenges and findings Chattanooga (TN): University of Tennessee at Chattanooga; 2020.
90. Saied E, Hashem AH, Ali OM, Selim S, Almuhayawi MS, Elbahnasawy MAJL. Photocatalytic and antimicrobial activities of biosynthesized silver nanoparticles using Cytobacillus firmus. *Life*. 2022;12:1331. doi:10.3390/life12091331
91. Kushwah M, Gaur M, Berlina AN, Arora K. Biosynthesis of novel Ag@ Cu alloy NPs for enhancement of methylene blue photocatalytic activity and antibacterial activity. *Mater Res Express*. 2019;6:116561.
92. Abbasi BH, Zaka M, Hashmi SS, Khan Z. Biogenic synthesis of Au, Ag and Au–Ag alloy nanoparticles using Cannabis sativa leaf extract. *IET Nanobiotechnol*. 2018;12:277–284.
93. Baptista PV, McCusker MP, Carvalho A, et al. Nano-Strategies to Fight Multidrug Resistant Bacteria-"A Battle of the Titans". *Front Microbiol*. 2018;9:1441. doi:10.3389/fmicb.2018.01441
94. Arora N, Thangavelu K, Karanikolos GN. Bimetallic Nanoparticles for Antimicrobial Applications. *Front Chem*. 2020;8:412. doi:10.3389/fchem.2020.00412
95. Zhang L, Jiang Y, Ding Y, Povey M, Yor D. Investigation into the antibacterial behaviour of suspensions of ZnO nanoparticles (ZnO nanofluids). *J Nanopart Res*. 2007;9:479–489.
96. Thirumoorthy G, Balasubramanian B, George JA, et al. Phytofabricated bimetallic synthesis of silver-copper nanoparticles using Aerva lanata extract to evaluate their potential cytotoxic and antimicrobial activities. *Sci Rep*. 2024;14(1):1270. doi:10.1038/s41598-024-51647-x
97. Vasiliev G, Kubo A-L, Vija H, et al. Synergistic antibacterial effect of copper and silver nanoparticles and their mechanism of action. *Sci Rep*. 2023;13(1):9202. doi:10.1038/s41598-023-36460-2

98. Jankauskaitė V, Vitkauskienė A, Lazauskas A, Baltrusaitis J, Prosyčevas I, Andrulevičius M. Bactericidal effect of graphene oxide/Cu/Ag nanoderivatives against Escherichia coli, Pseudomonas aeruginosa, Klebsiella pneumoniae, Staphylococcus aureus and Methicillin-resistant Staphylococcus aureus. *Int J Pharm*. 2016;511(1):90–97. doi:10.1016/j.ijpharm.2016.06.121
99. Huang X, Li T, Zhang X, Deng J, Yin X. Bimetallic palladium@ copper nanoparticles: Lethal effect on the gram-negative bacterium Pseudomonas aeruginosa. *Materials Science and Engineering: C*. 2021;129:112392. doi:10.1016/j.msec.2021.112392
100. Tabassum N, Khan F, Jeong GJ, Oh D, Kim YM. Antibiofilm and antivirulence activities of laminarin-gold nanoparticles in standard and host-mimicking media. *Appl Microbiol Biotechnol*. 2024;108:203.
101. Kang M-G, Khan F, Jo D-M, Oh D, Tabassum N, Kim Y-M. Antibiofilm and Antivirulence Activities of Gold and Zinc Oxide Nanoparticles Synthesized from Kimchi-Isolated Leuconostoc sp. Strain C2. *Antibiotics*. 2022;11(11):1524. doi:10.3390/antibiotics11111524
102. Alzohairy MA, Alzohairy MA, Alomary MN, et al. Effect of Biosynthesized ZnO Nanoparticles on Multi-Drug Resistant Pseudomonas Aeruginosa. *Antibiotics*. 2020;9(5):260. doi:10.3390/antibiotics9050260
103. Najafi M, Moghaddam M, Yousefi E. The Effect of Silver Nanoparticles on Pyocyanin Production of Pseudomonas aeruginosa Isolated From Clinical Specimens. *Avicenna J Med Biotechnol*. 2021;13(2):98–103. doi:10.18502/ajmb.v13i2.5529
104. Khan F, Manivasagan P, Lee J-W, Pham DTN, Oh J, Kim Y-M. Fucoidan-Stabilized Gold Nanoparticle-Mediated Biofilm Inhibition, Attenuation of Virulence and Motility Properties in Pseudomonas aeruginosa PAO1. *Mar Drugs*. 2019;17(4):208. doi:10.3390/md17040208
105. Mahmood H. Green synthesis of gold nanoparticles and their effect on pyocyanin pigment production from local Pseudomonas aeruginosa isolates. *Annals of the Romanian Society for Cell Biology*. 2021;25(1):6737–6748.
106. Jabłońska J, Dubrowska K, Augustyniak A, et al. Basic physiology of Pseudomonas aeruginosa contacted with carbon nanocomposites. *Appl Nanosci*. 2022;12:1929–1940.
107. Ali SG, Ansari MA, Khan HM, Jalal M, Mahdi AA, Cameotra SS. Crataeva nurvala nanoparticles inhibit virulence factors and biofilm formation in clinical isolates of Pseudomonas aeruginosa. *J Basic Microbiol*. 2017;57(3):193–203. doi:10.1002/jobm.201600175
108. Das MC, Sandhu P, Gupta P, et al. Attenuation of Pseudomonas aeruginosa biofilm formation by Vitexin: a combinatorial study with azithromycin and gentamicin. *Sci Rep*. 2016;6:23347. doi:10.1038/srep23347
109. Sandri A, Lleo MM, Signoretto C, Boaretti M, Boschi F. Protease inhibitors elicit anti-inflammatory effects in CF mice with Pseudomonas aeruginosa acute lung infection. *Clin Exp Immunol*. 2021;203(1):87–95. doi:10.1111/cei.13518
110. Kang D, Revtovich AV, Chen Q, Shah KN, Cannon CL, Kirienko NV. Pyoverdine-Dependent Virulence of Pseudomonas aeruginosa Isolates From Cystic Fibrosis Patients. *Front Microbiol*. 2019;10:2048. doi:10.3389/fmicb.2019.02048
111. Tabassum N, Khan F, Jeong G-J, Jo D-M, Kim Y-M. Silver nanoparticles synthesized from Pseudomonas aeruginosa pyoverdine: antibiofilm and antivirulence agents. *Biofilm*. 2024;7:100192. doi:10.1016/j.bioflm.2024.100192
112. Mohanty A, Liu Y, Yang L, Cao B. Extracellular biogenic nanomaterials inhibit pyoverdine production in Pseudomonas aeruginosa: a novel insight into impacts of metal(loid)s on environmental bacteria. *Appl Microbiol Biotechnol*. 2015;99(4):1957–1966. doi:10.1007/s00253-014-6097-5
113. Kirienko DR, Kang D, Kirienko NV. Novel Pyoverdine Inhibitors Mitigate Pseudomonas aeruginosa Pathogenesis. *Front Microbiol*. 2019;9:3317. doi:10.3389/fmicb.2018.03317
114. Fekete-Kertész I, Berkl Z, Buda K, Fenyvesi É, Szente L, Molnár M. Quorum quenching effect of cyclodextrins on the pyocyanin and pyoverdine production of Pseudomonas aeruginosa. *Appl Microbiol Biotechnol*. 2024;108(1):271. doi:10.1007/s00253-024-13104-7
115. Gajera G, Thakkar N, Godse C, DeSouza A, Mehta D, Kothari V. Sub-lethal concentration of a colloidal nanosilver formulation (Silversol®) triggers dysregulation of iron homeostasis and nitrogen metabolism in multidrug resistant Pseudomonas aeruginosa. *BMC Microbiol*. 2023;23(1):303. doi:10.1186/s12866-023-03062-x
116. Ghosh S, Jagtap S, More P, et al. Dioscorea bulbifera mediated synthesis of novel AucoreAgshell nanoparticles with potent antibiofilm and antileishmanial activity. *Journal of Nanomaterials*. 2015;2015:562938. doi:10.1155/2015/562938
117. Ioset J-R, Brun R, Wenzler T, Kaiser M, Yardley V. Drug Screening for Kinetoplastid Diseases: A Training Manual for Screening in Neglected Diseases. *DNDi and Pan-Asian Screening Network*. 2009:74.
118. Makada H, Habib S, Singh M. Bimetallic nanoparticles as suitable nanocarriers in cancer therapy. *Scientific African*. 2023;20:e01700. doi:10.1016/j.sciaf.2023.e01700
119. Ali S, Sharma AS, Ahmad W, et al. Noble Metals Based Bimetallic and Trimetallic Nanoparticles: controlled Synthesis, Antimicrobial and Anticancer Applications. *Crit Rev Anal Chem*. 2021;51(5):454–481. doi:10.1080/10408347.2020.1743964
120. Medina-Cruz D, Saleh B, Lomelí-Marroquín D, et al. Racing for the Surface. *Antimicrob Interface Tissue Eng*. 2020;2020:397–434.